

ABSTRACT

Title of Thesis: *EXAMINING HIBERNATION IN THE BIG BROWN BAT THROUGH DNA METHYLATION*

Isabel Rachel Sullivan, Master of Science, 2021

Thesis Directed by: Gerald S. Wilkinson, Professor of Biology

Hibernation allows individuals to conserve energy during seasonal low temperatures. As the physiological regulation of hibernation is inadequately understood, I examine hibernation using DNA methylation (DNAm). DNAm is the addition of a methyl group to cytosine at cytosine guanine dinucleotide (CpG) sites in the genome. DNAm in promoters can repress gene expression and be influenced by histone modifications. Using the big brown bat, *Eptesicus fuscus*, I examined how hibernation influences DNAm, independent of age, through comparing DNAm from bats that differed in hibernation history and comparing DNAm from the same individual between hibernating and active seasons. Both comparisons found evidence of differential enrichment of genes near significant CpG sites resulting from hibernation. The latter analysis found evidence consistent with a histone mark, associated with active transcription, is likely enriched in hibernating bats. These results suggest that DNAm and histone modifications associated with transcription factor binding regulate gene expression during hibernation.

EXAMINING HIBERNATION IN THE BIG BROWN BAT THROUGH DNA
METHYLATION

By

Isabel Rachel Sullivan

Thesis submitted to the Faculty of the Graduate School of the
University of Maryland, College Park, in partial fulfillment
of the requirements for the degree of
Master of Science
2021

Advisory Committee:

Professor Gerald S. Wilkinson, Chair

Assoc. Professor Stephen Mount

Assist. Professor Philip Johnson

© Copyright by
[Isabel Rachel Sullivan]
[2021]

Acknowledgements

I would like to acknowledge my collaborators Dr. Paul Faure and Lucas Greville at McMaster University, Dr. Lisa Cooper, Dr. Jeffrey Wenstrup, Dr. Alexander Galazyuk, and Inga Kristaponyte at NEOMed, and Dr. Steve Horvath and his group at UCLA. I also want to thank those who provided funding for this research, the American Society of Mammalogists, Sigma Xi, and the University of Maryland Graduate Student Government. This work would not have been possible without the help of Dr. Gerald Wilkinson and the Wilkinson Lab, specifically Danielle Adams for her assistance throughout this entire process. I also want to thank my fellow MEES students and Barry Bowman for your continued support. Finally, thank you to Hermes, Artemis, Hunter, Dopey, and Puff for making working from home more interesting.

Table of Contents

Acknowledgements	ii
Table of Contents	iii
List of Tables	iv
List of Figures	v
Introduction	1
Methods	6
Results	13
Discussion	19
Conclusion	26
Table 1	27
Figure 1	29
Figure 2	30
Figure 3	32
Figure 4	33
Figure 5	34
Figure 6	35
Figure 7	37
Figure 8	38
Figure 9	39
Figure 10	40
Appendix A	41
Appendix B	45
Appendix C	
Appendix D	
Bibliography	

List of Tables

Table 1 Hibernation-associated genes detected by DNAm change at CpG sites that show evidence of enrichment for histone marks in the cumulative hibernation (CH) and hibernation contrast (HC) analyses.

List of Figures

Figure 1. Histogram of hibernation opportunity (number of years exposed to cold winter temperatures divided by age) for all bats sampled in the summer. For the cumulative hibernation analysis, hibernation opportunity was coded 0, for bats under 5% (black) and 1 for bats greater than 5% (white).

Figure 2. Differentially methylated sites identified in the cumulative hibernation analysis with A) and B) illustrating the gene nearest two positive sites and C) and D) showing negative sites. Residual methylation refers to deviations from the value predicted by a least squares regression of DNAm beta on age for all samples.

Figure 3. The number of significant sites (inner circle) and non-significant sites (outer circle) for mapped positive and negative sites in the cumulative hibernation analysis.

Figure 4. Fold enrichment for the biological process classification in the cumulative hibernation analysis. The number on top of each bar indicates the number of genes in the *Eptesicus fuscus* background list for each process.

Figure 5. Evidence of histone enrichment obtained from eFORGE for the significant A) positive and B) negative sites identified in the cumulative hibernation analysis. Grey line and triangular symbols indicate significance (BY adjusted $P < 0.01$).

Figure 6. Differentially methylated sites identified in the hibernation contrast analysis with A) and B) illustrating the gene nearest two positive sites and C) and D) showing negative sites. Residual methylation refers to deviations from the value predicted by a least squares regression of DNAm beta on age for all samples.

Figure 7. The number of significant sites (inner circle) and non-significant sites (outer circle) for mapped positive and negative sites in the hibernation contrast analysis.

Figure 8. Fold enrichment for the biological process classification in the hibernation contrast analysis. The number on top of each bar indicates the number of genes in the *Eptesicus fuscus* background list for each process.

Figure 9. Evidence of histone enrichment obtained from eFORGE for the significant A) positive and B) negative sites identified in the hibernation contrast analysis. Grey line and triangular symbols indicate significance (BY adjusted $P < 0.01$).

Figure 10. Overlap in the number of significant, mapped CpG sites for A) age, cumulative hibernation (CH) and hibernation contrast (HC) analyses and B) for CH and HC analyses separated by sign. The asterisk indicates overlap that is significantly ($P < 0.05$) below expectation.

Introduction

Some endothermic animals can reduce their metabolism for short or long periods of time to conserve energy in response to changes in their environment (Pan et al., 2013; Jonasson and Willis, 2012; Andrews, 2019). Torpor is used to describe reduced body temperature and metabolic rate that lasts for a few hours or weeks. In contrast, hibernation consists of prolonged seasonal torpor bouts (Jastroch et al., 2016) interspersed between brief periods of arousal when body temperatures are increased to “active” levels (Blažek et al., 2019; Czenze et al., 2013). Animals in hibernation do not need to eat and have reduced metabolic rates without loss of muscle mass (Fedorov et al., 2014), loss of neural function (Lei et al., 2014; Szereszewski and Storey, 2019), or extensive water loss through skin (Klüg-Baerwald and Brigham, 2017; Stead, 2013; Ben-Hamo et al., 2013). Hibernation involves a suite of physiological processes including modification of neural transcription, (Drew, Frare, and Rice, 2017; Rouble, Tessier, and Storey, 2014), shifts in metabolic energy sources, (Hindle and Martin, 2013; Hashimoto et al., 2002), and tolerance of lowered body temperatures (Willis, 2017; Dausman and Glos, 2015; Carey, Andrews, and Martin, 2003). However, most of the genetic mechanisms regulating these processes are poorly understood and studied in few species (Al-attar and Storey, 2020; Grabek et al., 2015).

One method of identifying physiological mechanisms associated with hibernation is to compare gene expression in tissues taken from hibernating and nonhibernating individuals. Lists of differentially expressed genes can then be compared to a reference list to identify genetic pathways involved in hibernation. Such gene enrichment and other studies have found that hibernation protects skeletal muscle from atrophy (Tessier and Storey, 2014; Fedorov et al., 2014), inhibits immune function (Uzenbaeva et al., 2015;

Bouma et al., 2010), and suppresses metabolic function (Pan et al., 2013; Wu et al., 2016; Hindle and Martin, 2013; Hashimoto et al., 2002). Tissue-specific differences in gene expression have also been described between torpid and active animals. For example, genes associated with fat catabolism increased in expression during torpor in brown adipose tissue of thirteen-lined ground squirrels, *Ictidomys tridecemlineatus* (Hampton et al., 2013). Comparison of gene expression between torpid and active grizzly bears, *Ursus arctos horribilis* (Jansen et al., 2019) also revealed differences in several tissues. Brown adipose tissue had a three-fold reduction in expression of genes associated with fatty acid synthesis and cell growth but a 50% increase in expression of genes associated with glycolysis. For skeletal muscle, expression of genes associated with oxidative phosphorylation increased, but expression of genes associated with protein synthesis decreased during torpor. In the liver during torpor, circadian rhythm genes increased whereas expression of genes associated with insulin signaling decreased (Jansen et al., 2019). In the brains of torpid greater horseshoe bats (*Rhinolophus ferrumequinum*), expression of G-proteins, used for neuronal transmembrane signaling increased, but most proteins, including those associated with oxidative phosphorylation, decreased in expression in torpid bats (Yin et al., 2017).

Recently, DNA methylation (DNAm) has been used to examine the relationship between hibernation and regulation of gene expression (Alvarado et al., 2015; Biggar and Storey, 2014; Pinho et al., 2021). DNAm is the addition of a methyl group to a cytosine at cytosine guanine dinucleotides (CpG) sites (Moore et al., 2013). DNAm can suppress transcription through recruitment of transcriptional co-repressors and DNA methyltransferase enzymes (Biggar and Storey, 2014; Wade, 2001). DNAm can also interact with histone modifications to alter chromatin state and regulate gene expression (Rose and

Klose, 2014). By examining patterns of DNAm throughout the genome, inferences regarding elevated or repressed regulation of specific genes or gene pathways can be made (Razin & Riggs, 1980). DNAm can also provide insight into how gene expression is modified in response to environmental changes (Moore et al., 2013).

In addition to responding to some environmental effects, DNAm is well known to change with age. An overall decrease in global DNAm is typically observed as individuals get older (Unnikrishnan et al., 2018). However, some promoter regions show increases in DNAm over a lifetime (Rakyan et al., 2010). Those promoters are disproportionately associated with genes involved in development (Wang et al., 2020; Wilkinson et al., 2021). These DNAm patterns can be used to predict age with a high level of accuracy, an application known as an epigenetic clock (Horvath, 2013; Wilkinson et al., 2021). To create an epigenetic clock, DNAm quantified from known-aged individuals is used in a penalized regression to identify CpG sites that predict age (Horvath, 2013; Wilkinson et al., 2021). This method has recently been used to create a universal clock that works in multiple tissue from at least 128 mammal species (Lu et al., 2021)

Genome-wide and gene-specific patterns of DNAm have been examined in several hibernating rodent species. DNAm was profiled from yellow-bellied marmot (*Marmota flaviventer*) blood taken during active months. Using an epigenetic clock, they found that epigenetic age increased in the summer but remained constant throughout the winter. Additionally, they found of genes near CpG sites associated with season that were enriched for effects on metabolism, immune system, and circadian clock (Pinho et al., 2021). Global DNAm rates were examined in the liver, skeletal muscle (Alvarado et al., 2015), and brown adipose tissue (Biggar and Storey, 2014) of the thirteen-lined ground squirrel (*Ictidomys*

tridecemlineatus) at different points during hibernation. During torpor, DNAm decreased in liver and skeletal muscle and increased in brown adipose tissue (Alvarado et al., 2015; Biggar and Storey, 2014). DNAm has also been used to explore liver-specific transcription in a hibernation candidate gene (*HP-27*) in chipmunks (*Tamias asiaticus*). DNAm at an Upstream Stimulatory Factor (USF)-binding site, which partially regulates transcription of *HP-27*, was reduced in the liver but increased in the kidneys and heart (Fuji et al., 2006). A decrease in DNAm in the liver is consistent with activation of transcription for *HP-27*.

Determining if there are lineage-specific differences in hibernation processes requires comparison among multiple mammalian groups that undergo hibernation. As noted above, the majority of studies to date have involved rodents or carnivores. Many species of bats hibernate (Turbill, Bieber, and Ruf, 2011), but few studies have compared gene expression or DNAm between hibernating and nonhibernating individuals. In this study I used a relatively long-lived bat, *Eptesicus fuscus* (the big brown bat), to investigate the effect of hibernation on patterns of DNAm across the genome.

I examined the influence of hibernation on DNAm through two types of comparisons. The first comparison uses bats with different histories of hibernation. These bats fall into three categories: seasonally consistent hibernators, previous seasonal hibernators that are currently housed at constant temperatures, and those that have never experienced seasonal low temperatures. This analysis allows me to identify changes in DNAm associated with multiple years of hibernation. The second comparison uses paired samples taken in the winter and summer from captive bats that undergo hibernation every year. This repeated measures design allows me to detect changes in individual DNAm patterns directly resulting from hibernation. For each analysis, I corrected for age effects and

then compared methylation patterns between hibernation situations, identified CpG sites that are indicative of hibernation status after multiple testing, and conducted enrichment tests to identify biological processes and functional groups. I hypothesize that DNAm change at some CpG sites will differ between hibernators and non-hibernators independent of age. I also hypothesize that change in DNAm will be reduced in bats with a greater history of hibernation given that hibernation is a predictor of longevity in bats (Wilkinson and South, 2002; Wilkinson and Adams, 2019) and rate of change in DNAm is lower for long-lived bat species than for short-lived bat species (Wilkinson et al., 2021). I predict that CpG sites with elevated DNAm during hibernation will be enriched for genes associated with metabolism and immune system functioning. Results from these analyses should reveal if methylation patterns are influenced by single or repeated episodes of hibernation in *Eptesicus fuscus* and provide insight into the mechanisms used by bats for regulating physiological processes during hibernation.

Methods

Animal sources

Three captive *Eptesicus fuscus* groups that vary in their past opportunities for hibernation were used in this study. The first group is from the Cooper Laboratory at Northeast Ohio Medical University (NEOMed). These bats were either captured in 2005 in North Carolina or are descendants of those bats. They were initially kept at the University of Washington (Monroy et al., 2011) where the bats were maintained in an indoor-outdoor enclosure (Wilkinson et al., 2021). In 2014, the bats were moved to their current location in Ohio where they are kept indoors at an average temperature of 24°C on a 12-hour light/dark cycle. Thus, this colony includes older bats that could have undergone hibernation each winter in Washington as well as bats born in Ohio that have never experienced reduced winter temperatures. Because these animals were banded at capture or at birth, the hibernation history and age of each individual is known. Age ranges from 0.3 to 18.3 years. Ten samples were collected postmortem from individuals that were stored at -20°C since death. A total of 42 individuals were sampled from this source in the summer of 2018.

The second group is also kept at NEOMed and contains bats captured in Ohio either as juveniles or adults. These bats are kept indoors at an average temperature of 22°C. A total of 24 bats from this source were sampled in the summer of 2020.

The third group is housed at McMaster University in Hamilton, Ontario in an indoor-outdoor enclosure. In the summer, the enclosure temperature varies with ambient temperature. In the winter, a heater keeps the temperature in the indoor enclosure above 7°C. Minimum ages are available for wild caught individuals (6 bats) and exact ages for animals born in captivity (18 bats). Ages range from 0.7 to 10.1 years of age. In February,

2020, eight individuals were sampled in this colony. In July, 2020, 16 additional individuals were sampled, eight of which were the same bats sampled in February.

DNA Extraction

One or two 3 or 4 mm diameter tissue biopsies were taken from the wing of each bat by colleagues at each site (IACUC: 1213910-2). This is a noninvasive method of collecting tissue as wing punches typically heal in two weeks (Faure et al., 2009). In addition, wing tissue is composed of multiple tissue types i.e. skin, muscle, and blood (Cheney et al., 2017), which makes it useful as a source of DNA for measuring methylation (Wilkinson et al., 2021).

I extracted genomic DNA from wing tissue using a Zymo Quick-DNA miniprep plus kit (ZymoResearch, Orange, CA, USA) using the standard tissue protocol. Once extracted, DNA concentration was estimated using a QuBit. Samples with at least 250 ng of DNA but at a concentration under 10ng/μl were concentrated using a Millipore 30kDa centrifugal filter.

Quantification of DNA methylation

DNA samples were sent to the UCLA Neuroscience Genomics core facility for DNAm quantification. After bisulfite conversion, samples were hybridized to a custom Illumina microarray (“HorvathMammalMethylChip40”) containing 37,500 probes of conserved 50 base pair sequences with terminal CpG sites. The microarray was designed to assay DNAm from any mammal using probes largely conserved across 62 mammal species (Arneson et al., 2021). Alignment of the microarray probe sequences to the *Eptesicus fuscus* genome (v.1.0.) identified 28,606 probes (Wilkinson et al., 2021) where the genomic

location of each CpG was determined. These locations were categorized as either distal intergenic, 3' UTR, 5' UTR, promoter region, exon, or intron depending on the location of the nearest transcription start site for annotated genes (cf. Wilkinson et al., 2021). Beta values, i.e. the proportion of DNA molecules methylated at each CpG site, were normalized using the SeSaME procedure (Zhou et al., 2018) to correct for bias or variation among plates.

Identifying CpG sites associated with hibernation

I tested for an effect of hibernation on DNAm at each CpG site in two ways. The first used only samples taken in the summer from individuals that had different histories with regard to their opportunity to hibernate. I refer to this effect as cumulative hibernation history. The second involved comparison of samples taken from the same individual during the hibernation period (mid-February) or after reproduction (mid-July). Below, I refer to this effect as hibernation contrast. Each of these analyses provides a ranked list of significant CpG sites. Examination of these lists can reveal if the sites are nonrandomly distributed in the genome with regard to genomic features or are enriched with respect to the nearest genes or putative gene regulatory regions.

Because DNAm is known to change with age, before testing for hibernation, I adjusted DNAm for age. This adjustment requires knowledge of the age of all individuals. With an epigenetic clock created by Wilkinson et al. (2021), using an elastic net regression, age was estimated for wild caught individuals (Horvath, 2013; Wilkinson et al., 2021). Chronological age from 60 known-aged individuals was regressed to beta values using “glmnet” in R (Friedman et al., 2010) and elastic net regression models were created with an alpha of 0.5. This alpha value was not optimized for model performance but rather the alpha

of 0.5 was chosen as it is the midpoint between Ridge and Lasso regression as per elastic net standards. A 10-fold cross-validation was used in the `cv.glmnet` function to define optimal penalty parameters in the training set (Wilkinson et al., 2021). I then used this regression to predict age of wild-caught individuals.

I then fit a linear model for DNAm on age using the `lm` function in R (R Core Team, 2020) to the age predictions made from the epigenetic clock for *Eptesicus fuscus* samples ($n = 90$) at each CpG site. The resulting residuals represent age-adjusted methylation values and were used in both analyses below to examine hibernation effects on DNAm.

Cumulative Hibernation

To assess the cumulative effect of hibernation on DNAm at each site, I assigned each sample to one of two hibernation categories. Bats that had little opportunity to hibernate (less than 5% of their lifetime) were coded 0 (31 bats) while bats that had opportunities to hibernate over 5% of their lifetime were coded 1 (50 bats) (Fig. 1). I used a 5% threshold to ensure that measurable changes resulting from hibernation could be detected. To examine the cumulative effect of hibernation, I used a t-test (`rstatix` package: Kassambara, 2020) to compare residual DNAm values of bats with an opportunity to hibernate to bats with little opportunity to hibernate.

I corrected for multiple testing by applying a BY false discovery rate (Benjamini and Yekutieli, 2001) to obtain adjusted p-values. Because increases or decreases in DNAm can have opposite effects on gene expression, I used the sign of the t-statistic to label sites as “positive” or “negative”. Positive indicates greater DNAm for bats with an opportunity to hibernate relative to same-aged individuals without the opportunity to hibernate, while negative indicates less DNAm for bats with an opportunity to hibernate.

Hibernation contrast

To detect seasonal changes in methylation associated with hibernation, I used a paired t-test (rstatix package: Kassambara, 2020) to compare winter and summer residual DNAm values measured from the same individual. I corrected for multiple testing by again applying a BY false discovery rate to obtain adjusted p-values and ranked sites separately by the sign of the paired t-statistic. Because the hibernation contrast compared DNAm in winter to DNAm in summer, positive sites had relatively higher DNAm in the winter than summer while negative sites had relatively lower DNAm in the winter than summer after adjusting for age.

Enrichment tests

I used PANTHER v. 16.0 (Mi et al., 2020) to test for enrichment of genes nearest positive and negative significant CpG sites from each hibernation analysis. As multiple probes on the HorvathMammalMethylChip40 array are sometimes located near the same gene, the sign associated with each gene was determined based on the number of positively and negatively associated CpG sites. Genes with a greater number of significant negative sites were considered to be “negatively associated” and genes with a greater number of positive sites were considered to be “positively associated”. If genes had an equal number of positive and negative CpG sites, they were not included in the analysis. Additionally, probes located in intergenic regions were not considered as these regions provide uncertain information about nearest genes. All mapped CpG sites not in intergenic regions in the *Eptesicus fuscus* genome annotation were used as the background for these analyses. Separate enrichment tests were conducted on the positively and negatively associated gene

lists using a Fisher's Exact test with a False Discovery Rate (FDR) less than 0.05 to identify enrichment for protein type, biological process, or molecular function.

I conducted a second enrichment analysis directly on significant CpG sites using experimentally derived Functional element Overlap analysis of ReGions from EWAS, eFORGE v2.0 (Breeze et al., 2019). The eFORGE program tests for enrichment of functional regulatory elements by identifying probe sequences as being associated with five different histone marks or 15 different chromatin states identified in over 100 cell lines from multiple tissue sources by the Epigenomics Roadmap Consortium (https://egg2.wustl.edu/roadmap/web_portal/). These histone mark associations are determined through overlap with DNase I hypersensitive sites (DHS), which are specific regions where chromatin is accessible for binding (Santa Pau, Real, and Valencia, 2014). By comparing significant CpG sites to known DHS hotspots with epigenome associations, eFORGE allows for tissue-specific enrichment tests of DNAm. Permutation tests are then run against the species genomic background to determine which functional elements occur nonrandomly (Breeze et al., 2019).

I conducted separate analyses for positive and negative sites identified from each hibernation analysis and used this sign when describing the eFORGE analyses. The eFORGE analysis used only sites with an adjusted p-value below 0.05 or the most significant 1,000 sites in each direction, as the analysis is limited to 1,000 sites and default settings with *E. fuscus* as the species background. As bat wing tissue is comprised of skin, elastin, muscle, and blood (Cheney et al., 2017), I only report results for cell lines derived from these tissues.

For significant histone marks enriched from the eFORGE analyses, the gene symbol and genomic location of each CpG site were identified for the cell line with the greatest enrichment. Orthologous genes in non-intergenic regions were examined using the NCBI gene database (<https://www.ncbi.nlm.nih.gov/gene>), through a literature search to determine gene functions and associations. Common gene ontologies of these genes were determined using the functional classification analysis in PANTHER v. 16.0 (Mi et al., 2020) with a Fisher's Exact test (FDR < 0.05).

Results

Age-associated Sites

The linear model for DNAm on age identified 3,738 significant (BY $p < 0.05$) mapped CpG sites in the *E. fuscus* genome of which 1,616 were negatively associated and 2,122 were positively associated, which is more positively associated sites than expected by chance ($X^2 = 8.39$, $P = 0.004$). In addition, 665 positive and 534 negative unmapped sites were significant.

Cumulative Hibernation

The cumulative hibernation analysis identified 3,015 significant (BY $p < 0.05$) mapped CpG sites of which more are negatively associated (2,100) than positively associated with hibernation (915) than expected by chance ($X^2 = 19.35$, $P = 1.09 \text{ e-}05$). An additional 919 sites (623 negative, 296 positive) unmapped in the *E. fuscus* genome were significant. At positive sites, bats with a history of hibernation have more DNAm than bats with no history of hibernation after adjusting for age (Fig. 2A, 2B). At negative sites, bats with a history of hibernation have less DNAm than bats with no history of hibernation after adjusting for age (Fig. 2C, 2D). Significant sites were found in all genomic regions (Fig. 3), and no genomic region was significantly enriched for positive ($X^2 = 8.13$, BY $p > 0.05$) or negative sites ($X^2 = 7.41$, BY $p > 0.05$). Positive sites were associated with 316 orthologous genes and negative sites were associated with 893 orthologous genes out of 4,509 orthologous genes annotated on the array.

Genes nearest significant positive sites were not enriched for any protein class, biological process, or molecular function. However, genes nearest significant negative sites

did show enrichment. Protein class was enriched for DNA-binding transcription factor subset into gene-specific transcriptional regulator. Molecular functions were enriched for 14 types nested within two general functions: transcription by RNA polymerase II and regulation of transcription by RNA polymerase II. The most significant functions within these nests were nucleic acid binding and transcription regulator activity. For biological process, 36 significant processes were nested within two general processes: RNA polymerase II cis-regulatory region sequence-specific DNA binding and DNA-binding transcription factor activity, RNA polymerase II-specific. The most significant processes within those categories were organic cyclic compound metabolic process and regulation of cellular biosynthetic process. Additionally, 12 of these processes were associated with metabolism (Fig 4).

In contrast to the analysis using nearest genes, positive CpG sites showed evidence of significant enrichment for H3K4me3 histone marks associated with 11 cell lines from blood, muscle, and skin (Fig 5A). Among 170 CpG sites identified in the most significant cell line (E089 cell fetal muscle trunk), 22 were nearest genes associated with transcription factors with 43 additional genes related to RNA polymerase II transcription activity and 46 were related to DNA-binding transcription factor activity, RNA polymerase II-specific (Appendix A). Furthermore, 16 genes were associated with metabolism and, more specifically, five genes, Basonuclin 2 (BNC2), LIM Domain Only 4 (LMO4), PPARG Coactivator 1 Alpha (PPARGC1A), Proteasome 20S Subunit Beta 7 (PSMB7), and RAR Related Orphan Receptor A (RORA) were associated with hibernation (Table 1). No evidence of histone mark enrichment was found for negative sites (Fig. 5B).

Hibernation Contrast

A total of 1,952 CpG sites mapped in the *E. fuscus* genome showed significant differences in DNAm across seasons after adjusting for age (paired t-tests, BY $p < 0.05$), with more positive sites (1,609) than negative sites (343) than expected ($X^2 = 665.17$, $P < 2.2e-16$). In addition, 503 positive and 179 negative unmapped sites were significant. Across the genome and regardless of age, dramatic changes in DNAm occur depending on the season (Fig. 6). Significant sites are not enriched for any particular genomic region for positive ($X^2 = 6.09$, BY $p > 0.50$), or negative sites ($X^2 = 14.05$, BY $p > 0.05$) (Fig.7). Positive sites are associated with 919 known, unique genes and negative sites are associated with 245 known, unique genes.

Tests for enrichment of genes near positive or negative CpG sites gave results that differed from the cumulative hibernation analysis. Genes nearest negative sites were not enriched for any protein class, biological process, or molecular function. In contrast, genes nearest positive sites did show evidence of enrichment. Enriched protein classes included DNA-binding transcription factor subset into homeodomain transcription factor and gene-specific transcriptional regulator. The molecular function enrichment found 17 significant functions nested within two general functions: RNA polymerase II cis-regulatory region sequence-specific DNA binding and DNA-binding transcription factor activity, RNA polymerase II-specific. The most significant functions from these nests were DNA-binding transcription factor activity and sequence-specific DNA binding. For biological process, 44 significant processes were nested within three general processes: development, regulation of transcription by RNA polymerase II, and transcription by RNA polymerase II. The most significant processes within those categories were anatomical structure development,

regulation of gene expression, and regulation of cellular biosynthetic process. Additionally, 14 processes were associated with metabolism (Fig. 8).

Enrichment analysis of regulatory regions using positive CpG sites indicated enrichment for histone mark H3K4me1 in one associated skin cell line (Fig 9A). For negative CpG sites, evidence of enrichment for H3K4me1 was found in nine associated cell lines from blood, muscle, and skin and for H3K4me3 was found in one skin cell line (Fig. 9B). The positive CpG sites, showing evidence of enrichment for H3K4me1 in the E057 skin cell line, were nearest genes that were transcription factors (43) and additional genes that were associated with DNA-binding transcription factor activity, RNA polymerase II-specific (39), and RNA polymerase II cis-regulatory region sequence-specific DNA binding (38) (Appendix B). Furthermore, 10 of these associated genes were associated with hibernation: CCR4-NOT Transcription Complex Subunit 1 (CNOT1), Cannabinoid receptor 1 (CNR1), FosB Proto-Oncogene, AP-1 Transcription Factor Subunit (FOSB), Glycogen Synthase Kinase 3 Beta (GSK3B), MAPK Associated Protein 1 (MAPKAP1), Nuclear Receptor Subfamily 4 Group A Member 2 (NR4A2), Oxoglutarate Dehydrogenase (OGDH), Staphylococcal Nuclease And Tudor Domain Containing 1 (SND1), Tropomyosin 3 (TPM3), Transient Receptor Potential Cation Channel Subfamily M Member 7 (TRPM7) (Table 1).

The negative CpG sites from the hibernation contrast analysis showed evidence of greatest enrichment for H3K4me1 in the E090 muscle cell line. Genes nearest these sites were involved in regulation of transcription by RNA polymerase II (38), RNA polymerase II cis-regulatory region sequence-specific DNA binding (23), forebrain pattern formation (16), and DNA-binding transcription factor (25) (Appendix C). Furthermore, four genes have

previously been associated with hibernation: Acetyl-CoA Carboxylase Alpha (ACACA), BNC2, Deltex E3 Ubiquitin Ligase 3 (DTX3), and Titin (TTN) (Table 1). Genes nearest negative CpG sites with evidence of enrichment for H3K4me3 in the skin cell line, included transcription factors (24), RNA polymerase II-specific (21), RNA polymerase II transcription regulatory region sequence-specific DNA binding (20), and dentate gyrus development (5) (Appendix D). Four of the associated genes, ACACA, DTX3, PPARGC1A, and TTN, have been associated with hibernation (Table 1).

Independence of differentially methylated CpG sites across analyses

Only, five mapped sites that were significant in both hibernation analyses overlap with age-associated sites ($X^2 = 10,227$, $P < 2.2e-16$), which is less than expected (Fig. 10A). With one site positively associated with age and four sites negatively associated with age, overlapping sites were not significantly associated by sign (Fisher's Exact, $P = 0.19$). The overlap among significant age-associated and cumulative hibernation sites was less than expected with 303 overlapping sites ($X^2 = 2805.9$, $P < 2.2e-16$). Of these sites, 150 were positively associated with age and 153 were negatively associated with age (Fisher's Exact, $P = 0.91$). The overlap among significant age-associated and hibernation contrast sites was also less than expected with 402 overlapping sites ($X^2 = 998.48$, $P < 2.2e-16$). More overlap occurs among negatively age-associated sites (324) than among positively age-associated sites (78) (Fisher's Exact, $P = 1.42e-38$).

Comparison of the 3,015 cumulative hibernation sites and the 1,952 hibernation contrast sites revealed significantly less overlap than expected ($X^2 = 4987.6$, $P < 2.2e-16$) with 101 sites shared and mapped in the *E. fuscus* genome (Fig. 10B). Those 101 sites correspond to 81 orthologous genes with 34 in exons, 11 in 5'UTR, 5 in 3'UTR, 4 in

promoters, 16 in introns, and 11 in intergenic regions. Of these 81 genes, 22 were positively associated and 59 were negatively associated with cumulative hibernation and 60 were positively associated and 21 were negatively associated with hibernation contrast (Fig. 10).

For significant sites in genic regions in both cumulative hibernation and hibernation contrast analyses, 11 associated genes were identified as transcription factors and 16 were associated with regulation of transcription by RNA polymerase II. An additional eight sites were nearest to hibernation-related genes: OGDH, TTN, ACACA, Decorin (DCN), Fragile X mental retardation syndrome-related protein 1 (FXR1), AT-Hook DNA Binding Motif Containing 1 (ADHC1), Nuclear Receptor Family 4 Group A Member 3 (NR4A3), Glycerol-3-Phosphate Dehydrogenase 2 (GPD2). Furthermore, 11 sites that were significant in both analyses were also significant in the eFORGE analysis that varied in sign across analyses (Table 1).

Discussion

As predicted, after either single or repeated episodes of hibernation significant changes in DNAm were detected at numerous sites in the genome of *Eptesicus fuscus*. While some of those changes occur at sites that also show evidence of age-related changes in DNAm, the majority occur at sites where DNAm does not vary with age. I found that the age-associated sites more often increased than decreased in DNAm with age. Even though DNAm typically declines with age (Unnikrishnan et al., 2018), this result is consistent with a recent study of DNAm in 26 species of bats using the same methods (Wilkinson et al., 2021). Sites that increased in DNAm with age were more often located in promoter regions of genes, where many are associated with development. In contrast, sites that decreased in DNAm were rarely found in promoter regions and showed no evidence of enrichment for any biological process, consistent with unpredictable global loss of DNAm (Zhang et al., 2008). Below I discuss how the results from the two different methods used provide insight into the genetic regulation of hibernation.

DNAm change as a consequence of hibernation history

The cumulative hibernation analysis revealed that bats with a history of hibernation exhibit differences in DNAm compared to bats with no history of hibernation. Negative sites were over twice as common as positive sites. Negative sites indicate reduced DNAm and, therefore, should have more open chromatin, allowing for more DNA binding, and increased transcriptional activity. Elevated gene expression has been observed in some studies on hibernating animals. For example, in the brains of the greater horseshoe bat (*Rhinolophus ferrumequinum*), signal transduction factors, such as G Protein Subunit Alpha O1 (GNAO1) and G Protein Subunit Beta 1 (GNB1) increased during torpor (Yin et al., 2017). Similarly

in the brains of thirteen-lined squirrels (*Ictidomys tridecemlineatus*), eukaryotic translation initiation factor 2a (EIF2a) protein was increased during torpor (Tessier and Storey, 2014). Significant CpG sites were found in all genome regions and only genes nearest significant negative sites were enriched for specific protein types, biological processes, and molecular functions. Many enriched biological processes were involved in metabolism, consistent with previous findings where shifts in metabolic processes occur in hibernators (Hindle and Martin, 2013; Hashimoto et al., 2002).

In contrast to the gene enrichment analysis, analysis of significant positive CpG sites found evidence of enrichment for one histone mark, H3K4me3, in 11 cell lines from blood, muscle, and skin tissues and no enrichment for any histone mark for negative sites. The lack of histone enrichment for negative sites may be due to few sites located in promoter regions.

H3K4me3 histone marks regulate transcription at promoters where they directly recruit chromatin-modifiers such as histone deacetylases and acetyltransferases (Bannister and Kouzarides, 2011). Additionally, these modifications can prevent binding to H3 which can decrease enhancer functioning (Outchkourov et al., 2013). As few significant positive CpG sites in the cumulative hibernation analysis were in promoter regions, evidence of enrichment for H3K4me3 suggests that these CpG sites have decreased enhancer functioning. Many of the nearest genes associated with CpG sites in the most significant cell line, which was derived from muscle tissue, are associated with metabolism, RNA polymerase II transcription activity, and DNA-binding transcription factor activity. One of the transcription factors, BNC2, identified by a significant CpG site in an intron has been associated with increased activity in the brain of torpid *Mus musculus* (Hrvatin et al., 2020). Muscles also have shown an increase in transcription factors such as forkhead box O3

(FOXO3a) during torpor (Wu and Storey, 2014). This increase in transcriptional activity is thought to be a protective mechanism for muscle as muscles do not atrophy during hibernation (Federov et al., 2014). While most studies compare samples taken during hibernation to samples taken during active seasons, the cumulative analysis tests for effects of hibernation over the lifetime of the individual, which makes it challenging to associate changes in transcriptional activity to changes in DNAm.

Nevertheless, while enrichment analyses for CpG sites or genes nearest CpG sites show different patterns of enrichment at positive and negative sites, the results align with transcriptional modifications required for hibernation. Hibernation requires both suppression and activation of transcription to maintain a torpid state. While certain genes are upregulated during torpor, most genes, such as peroxisome proliferator-activated receptor alpha 2 (PPARa2), a nuclear receptor (Tessier and Storey, 2014; Yin et al., 2017) and genes associated with glycolysis decrease in expression during torpor (Yin et al., 2017).

As individual *E. fuscus* were nonrandomly sampled from three different groups, uncontrolled factors such as environmental exposure prior to capture, differences in laboratory settings, and genetic lineages could contribute to some detected DNAm differences. However, individuals with a history of hibernation were present in all three groups, which limits the possibility that differences in rearing caused the cumulative effects of hibernation. Future experiments that manipulate hibernation histories of bats would provide additional insight.

DNAm change between active and hibernating states

The comparison of DNAm from samples taken during versus after hibernation revealed nearly five times as many sites with increased than decreased DNAm. This result is consistent with hibernators reducing activity of many genes, such as those involved in metabolism and immune function (Bouma et al., 2010, Hashimoto et al., 2002). Significant positive and negative sites occur in genomic regions in proportion to their presence in the *E. fuscus* probe annotation of the array, indicating no enrichment of genomic location.

The gene enrichment analysis of negative sites revealed no evidence of enrichment of any biological process. This was unsurprising given the small number of genes near negative sites. However, the gene enrichment analysis of significant positive sites found evidence of enrichment of RNA polymerase II transcription, DNA-binding transcription factors, and regulation of gene expression for type of protein, biological process, and molecular function. In particular, many metabolic processes were enriched, which is similar to prior work on changes throughout an individual during hibernation, where gene expression affected metabolic rate depression amongst other processes at tissue-specific levels (Szereszewski & Storey, 2019).

For positive CpG sites in this analysis, evidence of enrichment was found for only the “active” histone mark, H3K4me1, in one skin cell line. The H3K4me1 mark is associated with gene enhancers, which regulate cell-specific gene expression (Local et al., 2018) and binding of effector proteins (Calo and Wysocka, 2013). This binding serves to regulate transcription via chromatin manipulation or assembly of transcription machinery (Calo and Wysocka, 2013; Musselman et al., 2012). The CpG sites associated with the skin cell line enriched for H3K4me1 are near genes with DNA-binding transcription factor

activity and RNA polymerase II cis-regulatory region sequence-specific DNA binding. As skin undergoes modifications for protection from water loss during torpor (Klög-Baerwald and Brigham, 2017; Stead, 2013; Ben-Hamo et al., 2013), transcriptional activity is expected during hibernation for these modifications. One of the genes associated with sites enriched in this histone mark, NR4A2, is a transcription factor previously associated with hibernation. NR4A2 was found to decrease in brown adipose tissue of thirteen-lined squirrels (*Ictidomys tridecemlineatus*) during torpor. As this gene is nearest CpG sites associated with H3K4me1, this suggests a similarly important role in hibernation of *E. fuscus*.

CpG sites with reduced methylation in hibernating bats (negative sites) showed evidence of enrichment for H3K4me1 in cell lines from skin, blood, and muscle. However, H3K4me3 showed evidence of enrichment in one skin cell line. In the most enriched cell lines associated with H3K4me1 and H3K4me3, most of the genes associated with significant CpG sites are transcription factors or are involved in the regulation of transcription by RNA polymerase II or brain development. A balance of H3K4me3 and H3K4me1 enrichment allows for transcriptional regulation. CpG sites associated with muscle tissue had the greatest enrichment for H3K4me1, which is consistent with active regulation of transcription in the muscle during hibernation. Genes associated with protein biosynthesis were found to be overexpressed in the muscle of black bears (*Ursus americanus*) (Fedorov et al., 2014). The skin cell line enriched in H3K4me3 was also enriched in H3K4me1, consistent with transcriptional regulation to modify skin cells during hibernation.

DNAm resulting from hibernation differs between long-term and seasonal hibernation

Comparison of sites showing significant changes in DNAm in response to age or hibernation revealed less overlap than expected. Only 1% of significant hibernation sites are shared between age-associated and cumulative hibernation sites and 2% of significant hibernation sites overlap between age-associated and hibernation contrast sites. This differs from previous findings where season-associated CpG sites overlapped significantly with age for hibernating yellow-bellied marmots (*Marmota flaviventris*). While hibernation has been associated with longevity (Wilkinson and South, 2002; Wilkinson and Adams, 2019), this result suggests that the effects of hibernation on DNAm can be seen even after adjusting for age effects.

Comparisons across hibernation analyses revealed less overlap in significant CpG sites than expected, suggesting that these analyses are capturing different effects of hibernation on DNAm. Most of the overlapping significant sites exhibited greater methylation during hibernation in the hibernation contrast analysis, suggesting that genes associated with these sites likely have reduced expression during hibernation. Additionally, both analyses showed evidence of enrichment across tissue types when compared to histone marks from cell lines associated with significant CpG sites. Most previously identified hibernation-related genes found in both analyses that were associated with H3K4me3 enrichment across cell lines decrease in expression during torpor, consistent with H3K4me3 decreasing enhancer functioning. (Outchkourov et al., 2013).

Hibernation-related genes identified by putative association with histone enrichment that were positive for both analyses have been found in prior hibernation studies to decrease in expression during torpor while genes that were negative for both analyses have been

previously found to increase in expression during torpor, suggesting dynamic transcriptional activity in hibernators. The different expression patterns align with previous findings where transcription is differentially regulated across tissue types and across species resulting from hibernation (Tessier and Storey, 2014; Andrews, 2019). Muscle tissue associated with significant sites for both analyses had the greatest histone enrichment, yet the analyses differed in type of histone mark. The difference is likely due to how hibernation, either cumulative or seasonal, influenced muscle tissue in each analysis. Similarly, putative enrichment of histone marks differed slightly between analyses but overall are consistent with suppression of RNA polymerase II transcription and DNA transcription factors in bats that hibernate. One such transcription factor, LMO4, was identified by positive changes in DNAm in both analyses and was found to be downregulated during torpor in the brain of the golden-mantled ground squirrel (*Spermophilus lateralis*) (Williams et al., 2005). However, the hibernation contrast analysis found enrichment of an active histone mark for cell lines associated with significant CpG sites. H3K4me1 was enriched in RNA polymerase II activity during torpor, suggesting that transcription is differentially regulated in torpor.

The overlap of significant sites in both cumulative and seasonal analyses is consistent with hibernation research in other species. Across different species, four genes were downregulated in brown adipose tissue (Hampton et al., 2013), bone marrow (Cooper et al. 2016), skeletal muscle (Jansen et al., 2019), and across tissue types (Lin et al., 2020). Further, three genes were upregulated in brown adipose tissue (Hindle and Martin, 2013), heart (Vermillion et al., 2015), and muscle (Vermillion et al., 2015; Fedorov et al., 2014) of different species. Seasonal differences in DNA methylation near one gene, AHDC1, was found in the blood of yellow-bellied marmots (*Marmota flaviventris*) (Pinho et al. 2021).

Conclusion

This project contributes new knowledge regarding the effects of hibernation on DNA methylation. No prior study has examined bat hibernation using DNA methylation. By comparing bats with a history of hibernation to bats with no history of hibernation I assess the long-term effects of hibernation and by comparing samples taken from the same individual during hibernation and during the active season I assess the seasonal, short-term effects. Over both timescales I observed significant changes in DNA methylation. By examining the direction of change at these CpG sites and location of these sites within the genome, I was able to make inferences about how DNA methylation influences changes in gene expression associated with hibernation.

These results represent only the beginning of how DNAm can be used for understanding environmental impacts on animals. This work expands upon research examining hibernation affecting DNA methylation (Alvarado et al., 2015; Biggar and Storey, 2014; Pinho et al., 2021). Additional comparisons of DNA methylation patterns between long-lived and hibernating bats may provide insight into the relationship between aging and hibernation.

Table 1: Hibernation-associated genes detected by DNAm change at CpG sites that show evidence of enrichment for histone marks in the cumulative hibernation (CH) and hibernation contrast (HC) analyses

Gene Symbol	DNAm change		Histone Mark		Effect of torpor on gene	Source
	CH	HC	H3K4me1	H3K4me3		
ACACA	Negative	Negative		HC	Downregulated	Jansen et al., 2019
ACADVL	Positive			CH	Upregulated	Vermillion, et al., 2015
AHDC1	Negative	Positive	HC		Candidate	Pinho et al., 2021
BANP	Positive			HC	Downregulated	Andrews, 2019
BNC2*	Positive	Negative	HC	CH	Upregulated	Hrvatin et al., 2020
CLK1		Positive	HC		Downregulated	Andrews, 2019
CNOT1		Positive	HC		Downregulated	Capraro et al., 2020
CNR1		Positive	HC		Downregulated	Boyer et al., 2020
CRTC2		Positive	HC		Upregulated	Capraro et al., 2020
CTNNA3	Negative	Positive	HC		Upregulated	Capraro et al., 2019
DCN	Positive	Negative	HC	CH	Downregulated	Cooper et al., 2016
DHX40		Positive	HC		Candidate	Williams et al., 2020
DMD	Positive	Positive	HC	CH	Downregulated	Lin et al., 2020
DTX3	Negative	Negative		HC	Upregulated	Nespolo et al., 2018
FOSB*		Positive	HC		Upregulated	Fu et al., 2021
FXR1	Negative	Negative	HC		Upregulated	Fedorov et al., 2014
GPD2	Negative	Positive	HC		Upregulated	Hindle and Martin, 2013
GRIN2B	Negative	Positive	HC		Upregulated	Capraro et al., 2019
GSK3B		Positive	HC		Upregulated	Stieler et al., 2011
HOXA3*	Negative	Positive	HC		Downregulated	Capraro et al., 2019
LIN7C	Positive			CH	Upregulated	Crawford et al., 2007
LMO4*	Positive	Positive	HC	CH	Downregulated	Williams et al., 2005
MAPKAP1		Positive	HC		Upregulated	Luu et al., 2016
NQO1		Positive	HC		Upregulated	Yin et al., 2016

NR4A2*		Positive	HC		Downregulated	Hampton et al., 2013
OGDH		Positive	HC		Downregulated	Lin et al., 2020
PPARGC1A	Negative	Negative		HC	Downregulated	Capraro et al., 2020; Hampton et al., 2013
RORA	Positive			CH	Downregulated	Mugahid et al., 2019
SND1	Positive			CH	Candidate	Hindle and Martin, 2013
SRSF5	Negative	Positive	HC		Candidate	Fu et al., 2021
TOB2	Positive			CH	Downregulated	Fu et al., 2021
TPM3	Positive	Positive	HC	CH	Downregulated	Lin et al., 2020
TRPM7		Positive	HC		Upregulated	Cooper et al., 2016
TTN	Positive	Negative		CH, HC	Upregulated	Vermillion et al., 2015
ZNF451	Positive			CH	Candidate	Williams et al., 2020

* indicates transcription factors

Figure 1. Histogram of hibernation opportunity (number of years exposed to cold winter temperatures divided by age) for all bats sampled in the summer. For the cumulative hibernation analysis, hibernation opportunity was coded 0, for bats under 5% (black) and 1 for bats greater than 5% (white).

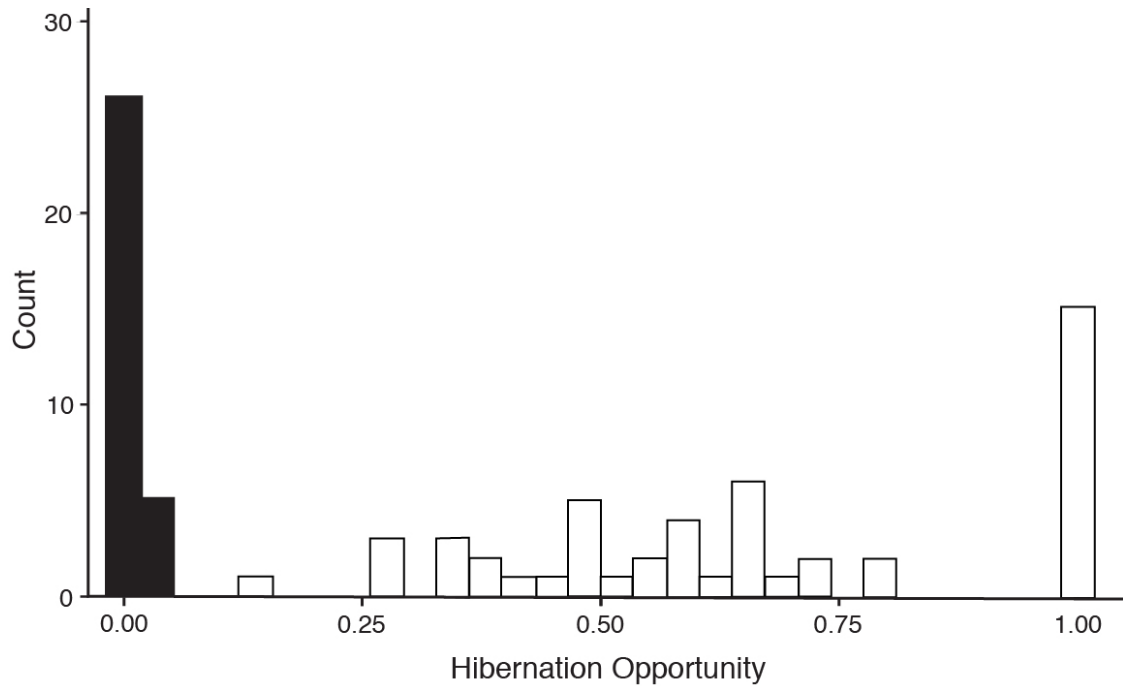


Figure 2

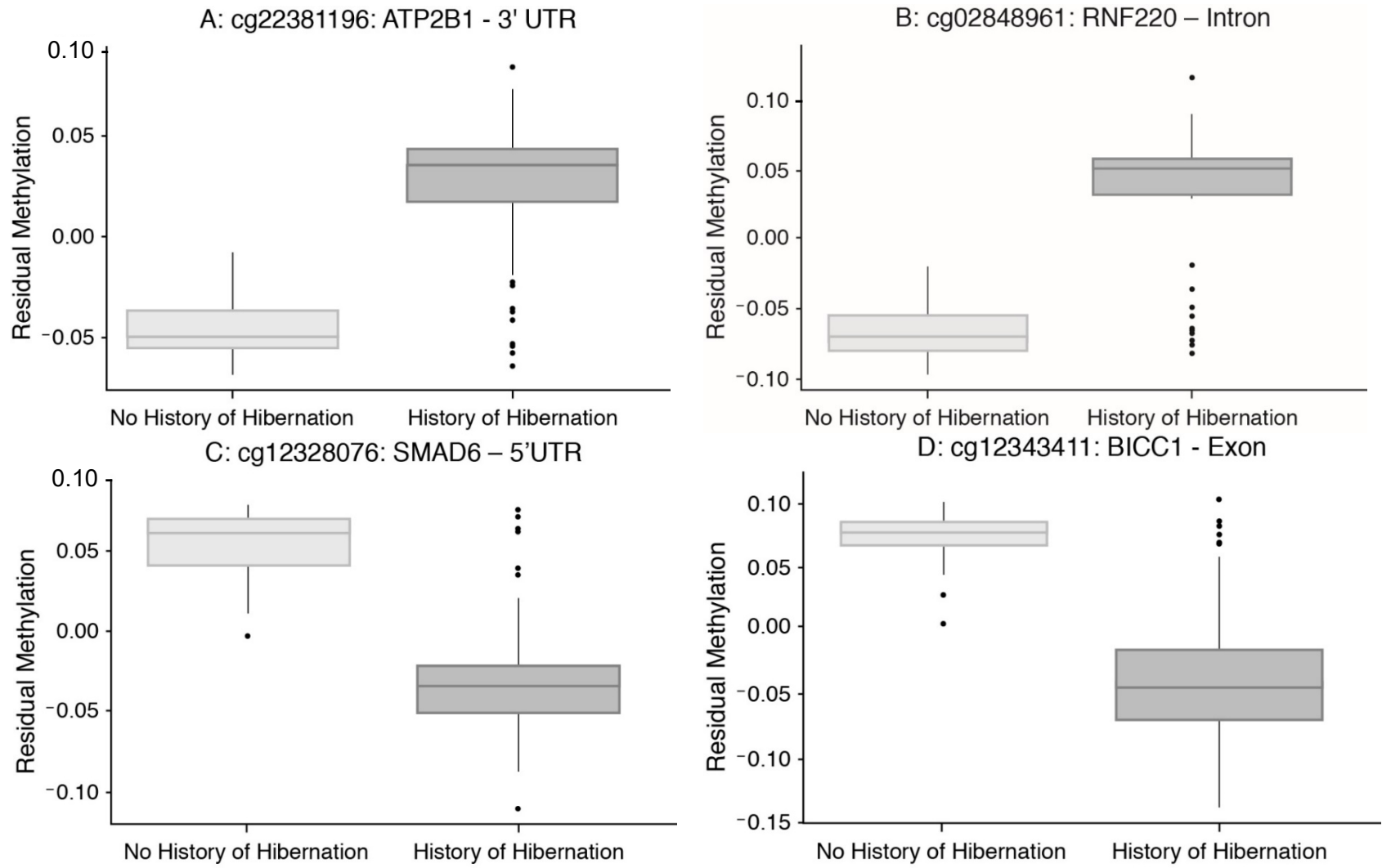


Figure 2. Differentially methylated sites identified in the cumulative hibernation analysis with A) and B) illustrating the gene nearest two positive sites and C) and D) showing negative sites. Residual methylation refers to deviations from the value predicted by a least squares regression of DNAm beta on age for all samples.

Figure 3. The number of significant sites (inner circle) and non-significant sites (outer circle) for mapped positive and negative sites in the cumulative hibernation analysis.

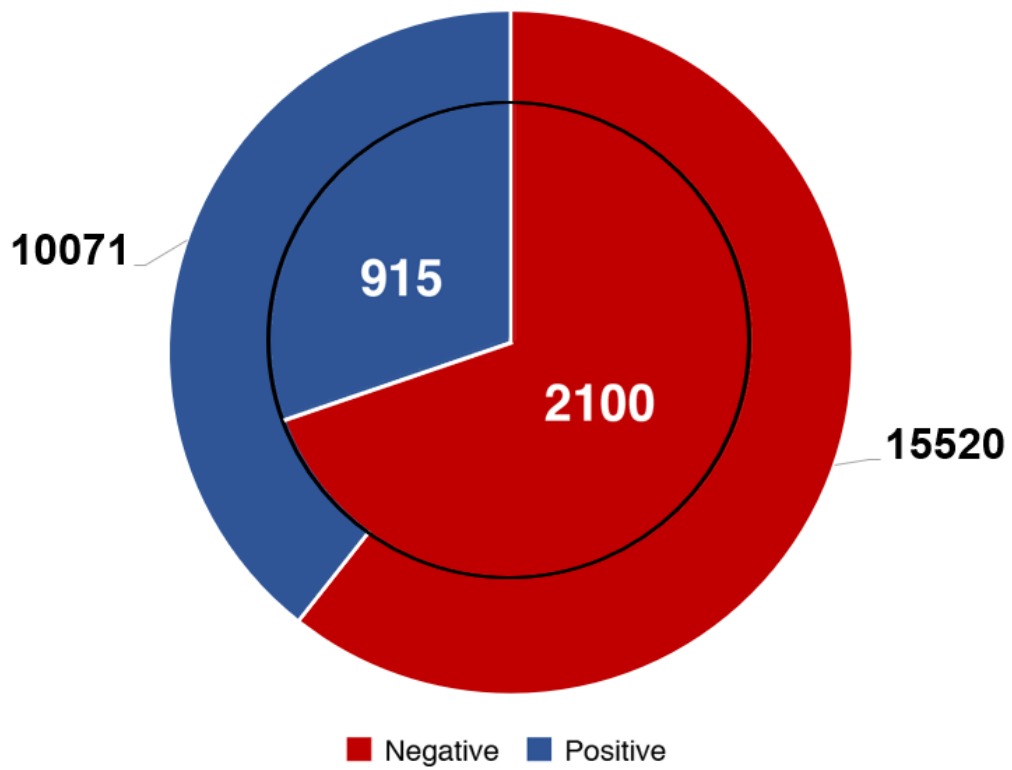


Figure 4. Fold enrichment for the biological process classification in the cumulative hibernation analysis. The number on top of each bar indicates the number of genes in the *Eptesicus fuscus* background list for each process.

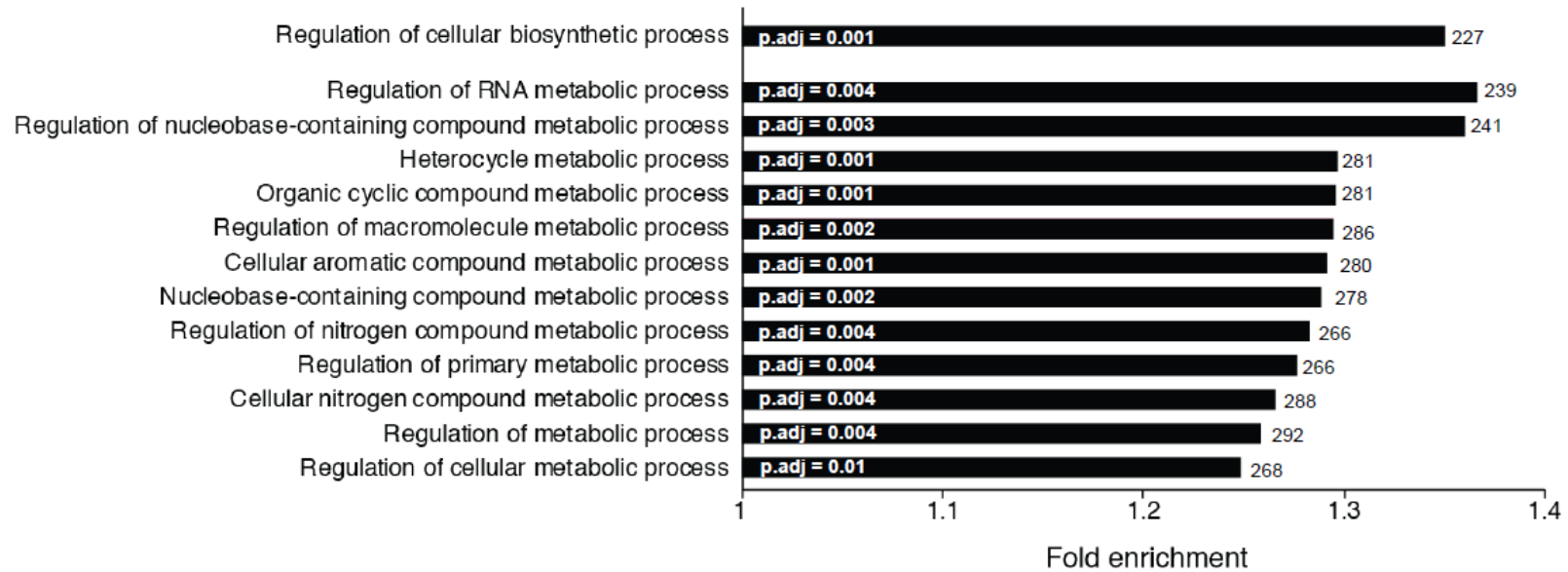


Figure 5. Evidence of histone enrichment obtained from eFORGE for the significant A) positive and B) negative sites identified in the cumulative hibernation analysis. Grey line and triangular symbols indicate significance (BY adjusted $P < 0.01$).

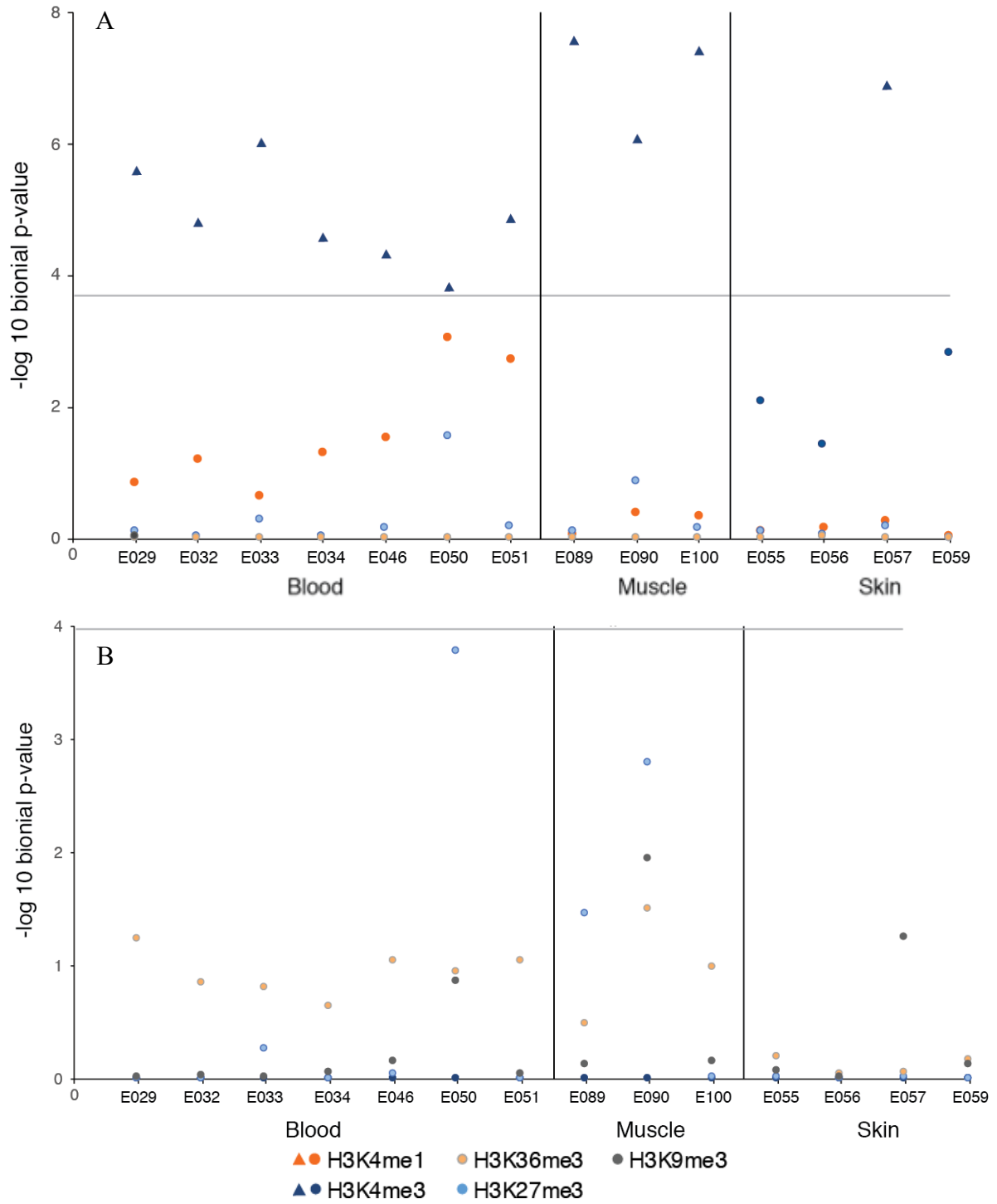


Figure 6

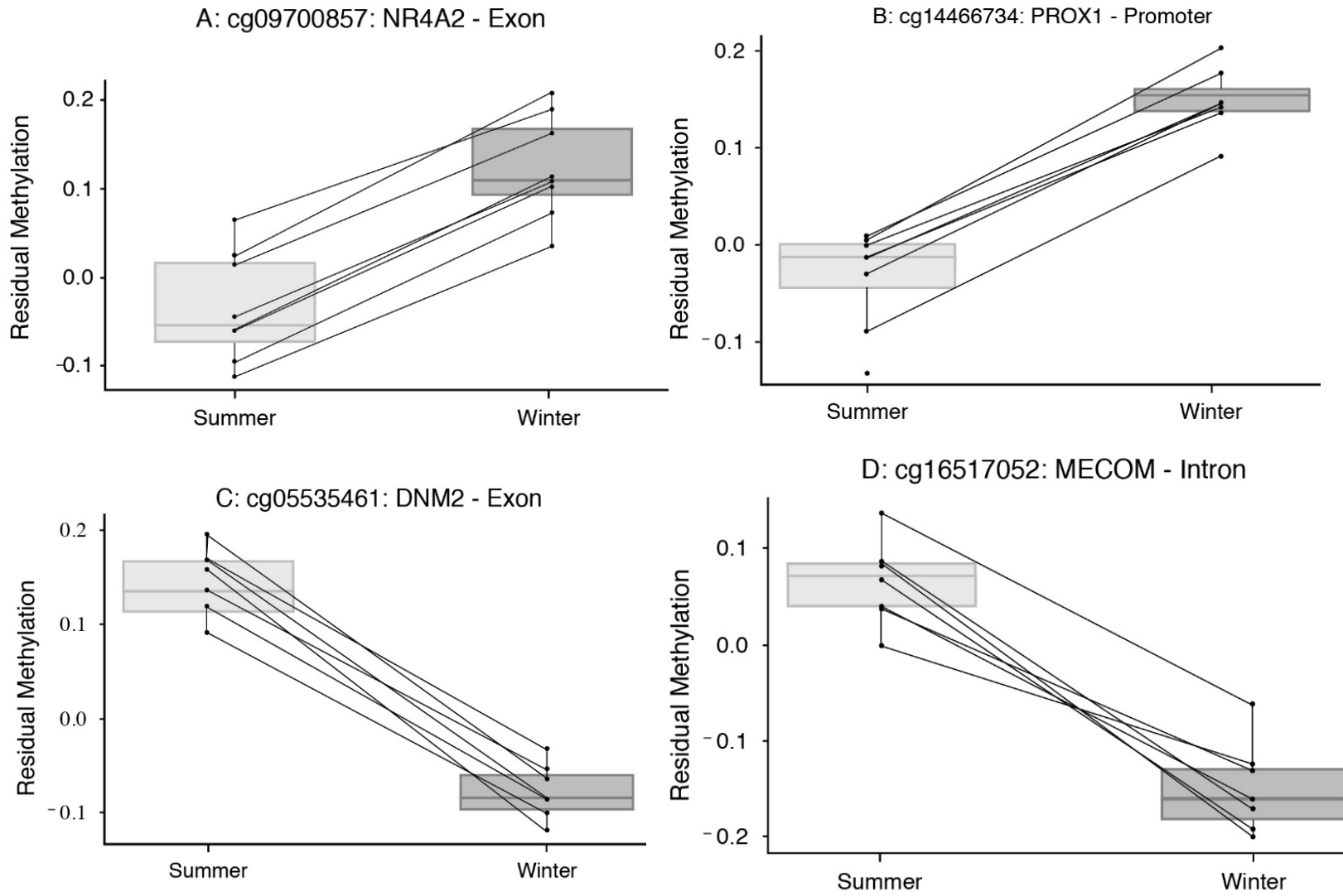


Figure 6. Differentially methylated sites identified in the hibernation contrast analysis with A) and B) illustrating the gene nearest two positive sites and C) and D) showing negative sites. Residual methylation refers to deviations from the value predicted by a least squares regression of DNAm beta on age for all samples.

Figure 7. The number of significant sites (inner circle) and non-significant sites (outer circle) for mapped positive and negative sites in the hibernation contrast analysis.

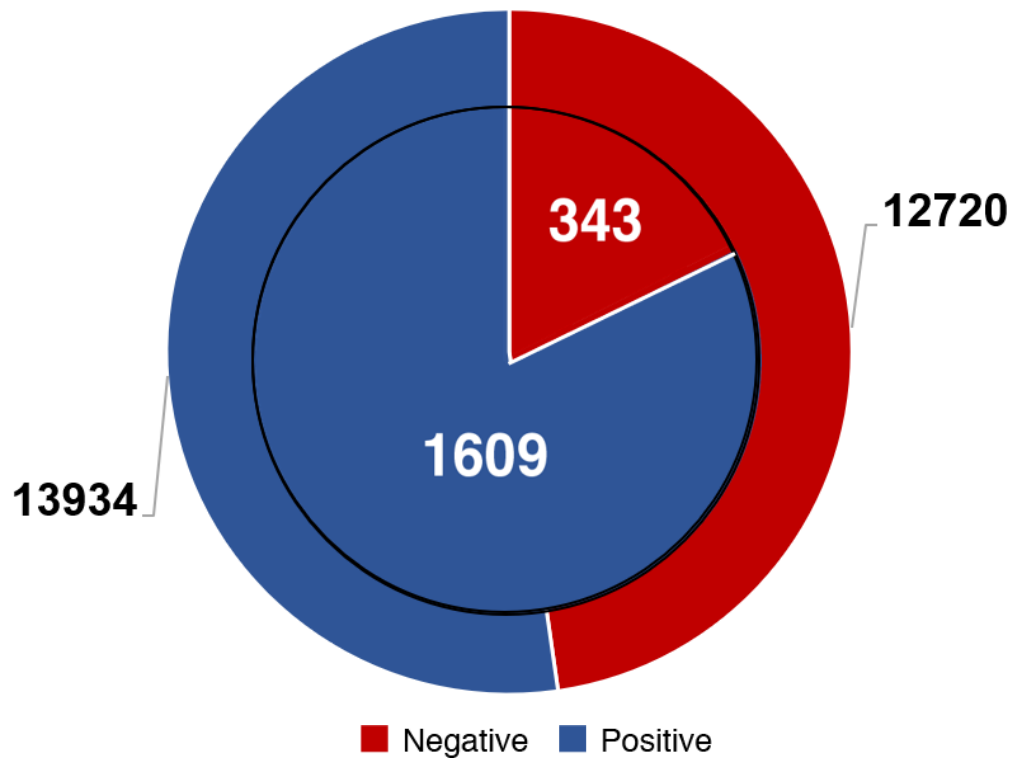


Figure 8. Fold enrichment for the biological process classification in the hibernation contrast analysis. The number on top of each bar indicates the number of genes in the *Eptesicus fuscus* background list for each process.

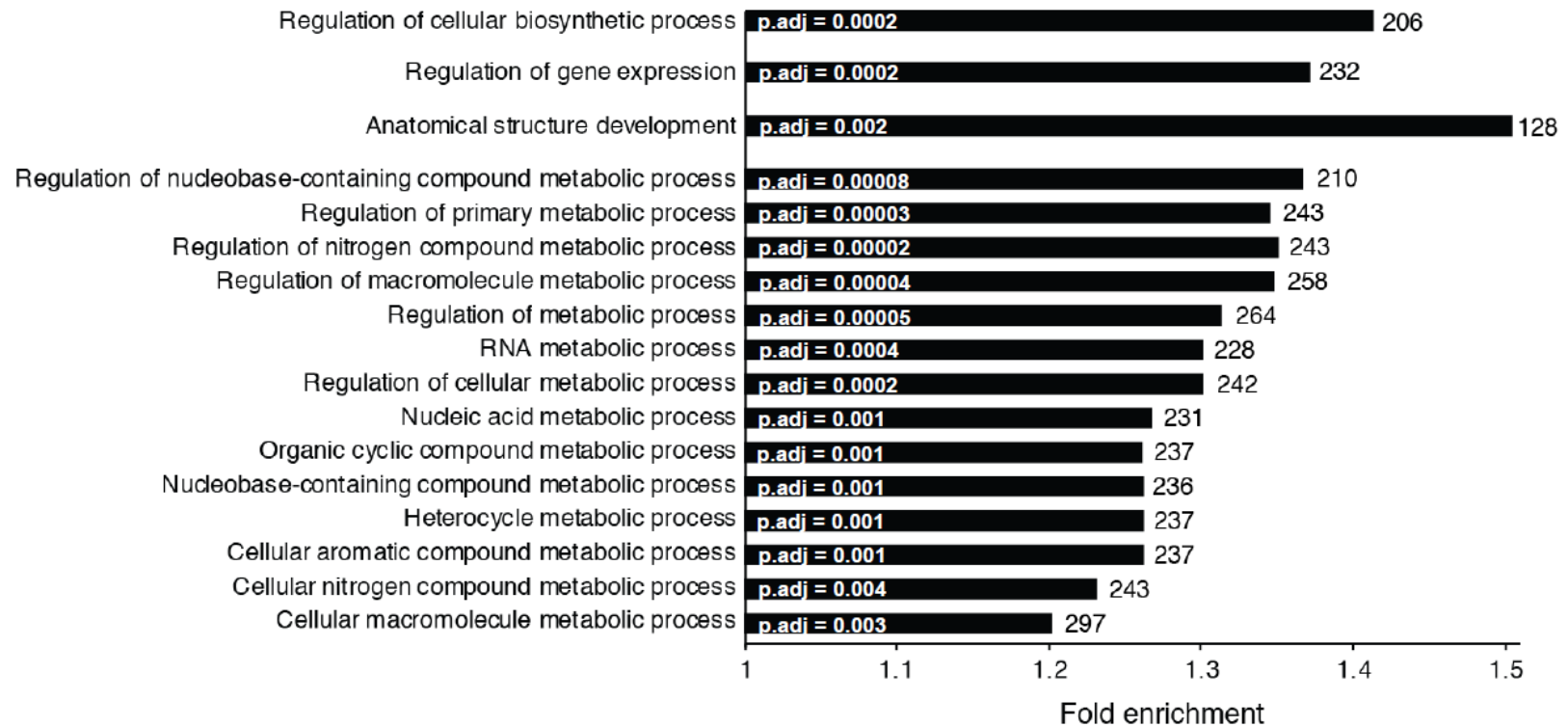


Figure 9. Evidence of histone enrichment obtained from eFORGE for the significant A) positive and B) negative sites identified in the hibernation contrast analysis. Grey line and triangular symbols indicate significance (BY adjusted $P < 0.01$).

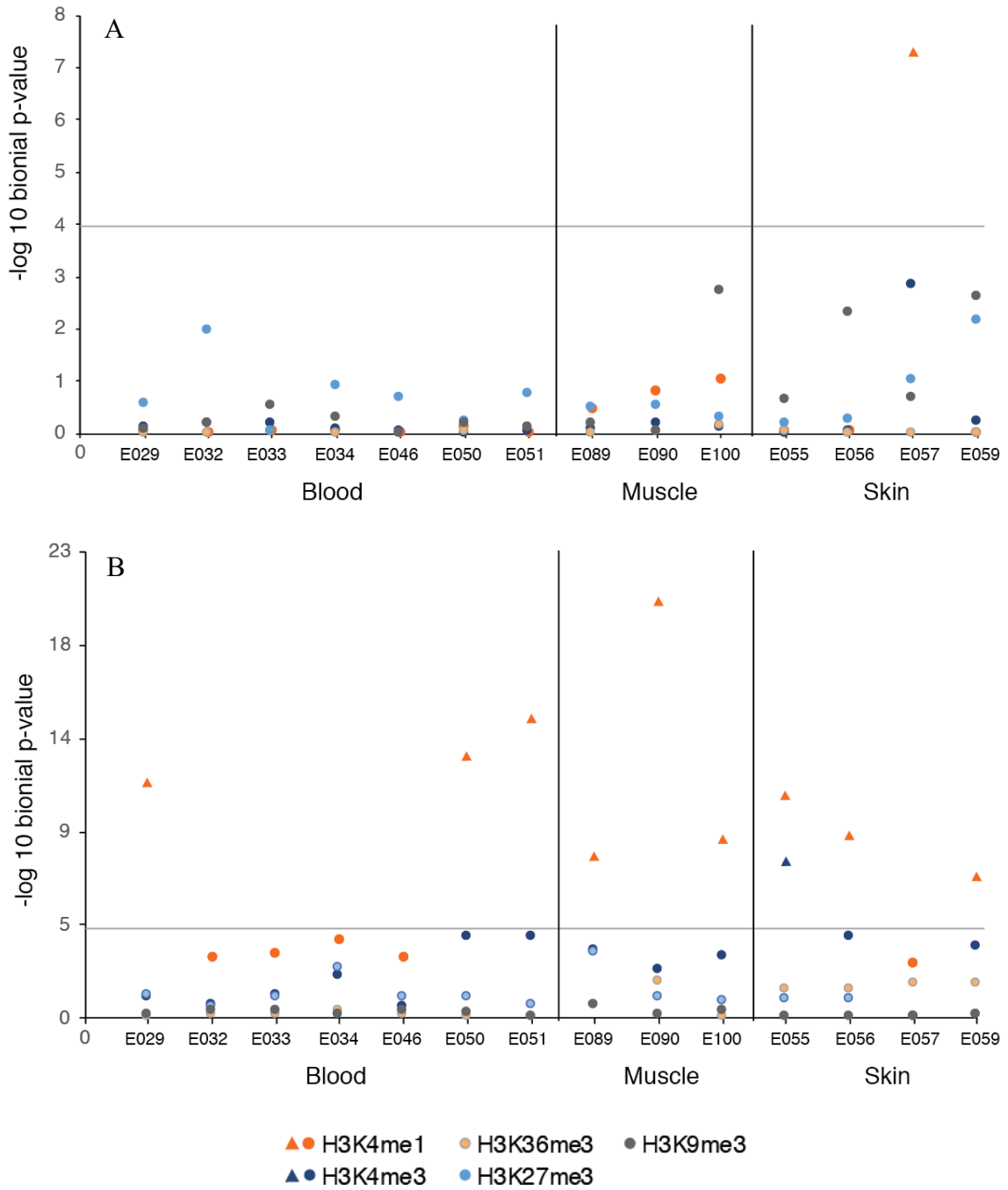
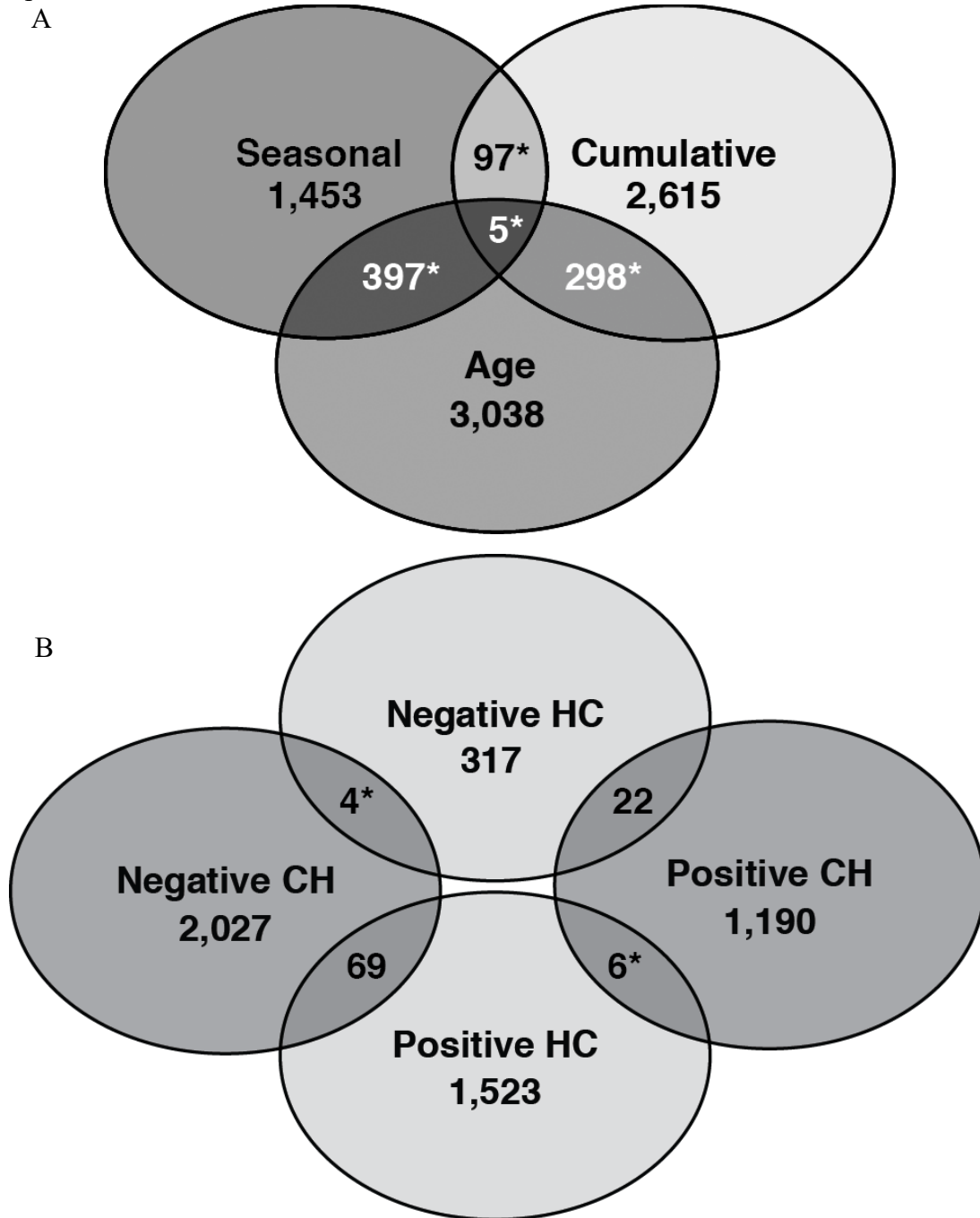


Figure 10. Overlap in the number of significant, mapped CpG sites for A) age, cumulative hibernation (CH), and hibernation contrast (HC) analyses and B) for CH and HC analyses separated by sign. The asterisk indicates overlap that is significantly ($P < 0.05$) below expectation



* = $P < 0.05$

Appendix A Positive CpG site associations in E089 cell fetal muscle trunk for the cumulative hibernation analysis

CpG site	Symbol	Location	Category
cg14471793	CCND2	Promoter	Signaling pathways
cg02530738	CDON	Promoter	Regulation of gene expression
cg06173215	HOXA11	Promoter	Regulation of transcription by RNA polymerase II, transcription factor
cg05853816	HOXA9	Promoter	Regulation of transcription by RNA polymerase II, transcription factor
cg07143052	LMO4	Promoter	Hibernation, regulation of transcription by RNA polymerase II, transcription factor
cg23050718	MN1	Promoter	Regulation of transcription by RNA polymerase II
cg06618394	NR2F2	Promoter	Transcription factor, Regulation of transcription by RNA polymerase II
cg09227056	SAMD4A	Promoter	polymerase II
cg20378060	SP8	Promoter	Regulation of cell motility
cg02522446	ZIC1	Promoter	Transcription factor, regulation of transcription by RNA polymerase II
cg25220579	BCL11B	Intron	Transcription factor, regulation of transcription by RNA polymerase II
cg21574349	BCOR	Intron	Regulation of gene expression, Histone methylation, to regulation of transcription by RNA polymerase II
cg18211931	BNC2	Intron	Hibernation, transcription factor
cg10588150	CFAP77	Intron	Structural protein
cg02580016	CSMD3	Intron	Dendrite development
cg13505775	CXXC5	Intron	Signaling pathways
cg14435709	DDX46	Intron	MRNA splicing
cg12956982	EBF1	Intron	Chromatin organization, regulation of transcription by RNA polymerase II
cg13228972	EPHA3	Intron	Signaling pathways
cg03924819	ERI3	Intron	DNA binding
cg24625070	FAM222B	Intron	Protein coding
cg09509790	FOXP1	Intron	Transcription factor, regulation of gene expression, neurotransmitter receptor activity, signaling pathways
cg02734933	HDAC9	Intron	Histone methylation, signaling pathways, chromatin organization
cg06149833	HMX3	Intron	Regulation of transcription by RNA polymerase II, transcription factor
cg22012813	HOXC4	Intron	Regulation of transcription by RNA polymerase II, transcription factor
cg02215945	LRBA	Intron	Cold adaptation
cg12564910	LRMDA	Intron	Melanocyte differentiation

cg06210673	MAP2K5	Intron	Signaling pathways, Metabolic processes
cg04493740	MECOM	Intron	Transcription factor, regulation of transcription by RNA polymerase II
cg19583117	MED23	Intron	Regulation of gene expression, transcription factor, regulation of gene expression
cg06410866	MEIS1	Intron	Hibernation, transcription factor, regulation of transcription by RNA polymerase II
cg07048205	MEIS2	Intron	Chromatin organization, transcription factor, regulation of transcription by RNA polymerase II
cg17203506	OGA	Intron	Hydrolase
cg27564792	PPARGC1A	Intron	Regulation of transcription by RNA polymerase II, circadian rhythm regulation of gene expression, hibernation, metabolic processes
cg11326290	PSMB7	Intron	Metabolic processes
cg05622324	RANBP17	Intron	Plays a key role in NLS-dependent protein import
cg23145794	SETD5	Intron	Histone methylation
cg03132556	SF1	Intron	DNA binding
cg08434263	SLIT3	Intron	Signaling pathways
cg00331190	SMOC1	Intron	Extracellular matrix organization
cg21417632	TMEM260	Intron	Protein coding
cg00234378	ACSS3	Exon	Methylcitrate cycle
cg02770072	ADNP	Exon	Regulation of gene expression
cg20243605	AGAP2	Exon	Metabolic processes
cg13842554	AGBL4	Exon	Metabolic processes
cg01784199	BEND3	Exon	Regulation of transcription by RNA polymerase II
cg22662148	CACNG4	Exon	Signaling pathways, metabolic processes
cg06734127	CADPS	Exon	Metabolic processes
cg09053298	CNOT9	Exon	Regulation of transcription by RNA polymerase II
cg01594821	CUNH16orf72	Exon	Protein coding
cg23327296	CXXC4	Exon	Signaling pathways
cg02569533	DSCAML1	Exon	Scaffold/adaptor protein
cg11219763	EIF3A	Exon	Translation initiation factor
cg23644927	EMSY	Exon	Chromatin organization, regulation of transcription by RNA polymerase II
cg04801716	GAS1	Exon	Signaling pathways
cg17378114	GNPTAB	Exon	Transcription factor
cg07459759	HOXD10	Exon	Regulation of transcription by RNA polymerase II, transcription factor

cg20415069	HOXD11	Exon	Transcription factor
cg02268145	KANSL2	Exon	Histone methylation
cg09067962	KCNC1	Exon	Transmembrane transport
cg01531512	KDM3B	Exon	Histone methylation, chromatin organization, regulation of transcription by RNA polymerase II
cg16372141	KDM5C	Exon	Histone methylation, chromatin organization, hibernation, transcriptional repression
cg09738329	KIAA1549L	Exon	VEGFR2 cascades
cg21249921	KMT2B	Exon	Histone methylation, regulation of transcription by RNA polymerase II
cg01614615	LARP1	Exon	Metabolic processes
cg12607756	MAP1LC3A	Exon	Metabolic processes
cg06794263	MARCHF3	Exon	Metabolic processes
cg03779905	MBTD1	Exon	Histone methylation, chromatin organization, transcriptional repression
cg06169648	METTL3	Exon	RNA methylation
cg24313007	NAV2	Exon	Neurotransmitter receptor activity
cg13613983	PAPOLA	Exon	Adenylyltransferase activity
cg26448296	PAX2	Exon	Chromatin organization, regulation of transcription by RNA polymerase II
cg20959523	PHLDB1	Exon	Cytoskeleton organization
cg21760034	PPFIA4	Exon	Neurotransmitter receptor activity
cg26047375	PPP1R3F	Exon	Metabolic processes
cg19904709	PTCHD1	Exon	Neurotransmitter receptor activity
cg09632916	PTPN4	Exon	Protein tyrosine phosphatase activity
cg03840462	RBBP6	Exon	Metabolic processes, cold adaptation
cg05454653	RBM27	Exon	Metabolic processes
cg20348846	RBM6	Exon	MRNA splicing
cg09267036	SIDT1	Exon	RNA transmembrane transporter activity
cg08659673	SMARCA1	Exon	Chromatin organization, signaling pathways, regulation of transcription by RNA polymerase II
cg01757860	SYNCRIP	Exon	Regulation of gene expression, metabolism
cg12798264	SYT7	Exon	Signaling pathways
cg09200766	TBRG1	Exon	Growth factors
cg01394860	TMEM151A	Exon	Protein coding
cg14992209	ZBTB7C	Exon	Regulation of transcription by RNA polymerase II
cg11785939	ZEB2	Exon	Signaling pathways, regulation of transcription by RNA polymerase II
cg08123193	ZFHX3	Exon	Signaling pathways, transcription factor

cg16788303	ZNF451	Exon	Metabolic processes, transcription factor, regulation of transcription by RNA polymerase II
cg27070699	CDK14	5'UTR	Regulation of transcription by RNA polymerase II
cg10593080	DLGAP4	5'UTR	Neurotransmitter receptor activity, metabolic processes
cg16209866	EVX1	5'UTR	Regulation of transcription by RNA polymerase II
cg24480093	NUFIP2	5'UTR	RNA binding
cg02679551	PTPRG	5'UTR	Protein dephosphorylation
cg19661431	TOP1	5'UTR	Chromatin organization
cg17571666	CSNK2A2	3'UTR	Signaling pathways
cg02601407	INSM1	3'UTR	Neurotransmitter receptor activity, regulation of Transcription by RNA polymerase II
cg23781022	ITGB7	3'UTR	Signaling pathways
cg14506140	RORA	3'UTR	Hibernation, regulation of transcription by RNA polymerase II
cg18876430	TCF7L2	3'UTR	Chromatin organization, transcription factor, signaling pathway, regulation of transcription by RNA polymerase II
cg07448217	TEAD1	3'UTR	Chromatin organization, transcription factor, signaling pathways, regulation of transcription by RNA polymerase II
cg21917532	ZNF827	3'UTR	Transcription factor, regulation of transcription by RNA polymerase II

Appendix B Positive CpG site associations in E057 foreskin keratin skin cell line for the hibernation contrast analysis

CpG site	Symbol	Location	Category
cg03848010	BCOR	Promoter	DNA-binding transcription factor activity, regulation of gene activity, chromatin organization
cg18020892	FAF1	Promoter	DNA-binding transcription factor activity
cg25974818	GLYR1	Promoter	Histone methylation, DNA-binding transcription factor activity
cg01631669	GRIA2	Promoter	Neurotransmitter receptor activity, signaling pathways
cg15797635	KIAA0825	Promoter	Protein coding
cg00256784	PBX3	Promoter	DNA-binding transcription factor activity, transcription factor
cg27230947	SRGAP2	Promoter	Neurotransmitter receptor activity, signaling pathways
cg04686121	TLX3	Promoter	DNA-binding transcription factor activity, immune system function, neurotransmitter receptor activity
cg08305575	ADD1	Intron	Extracellular matrix organization
cg09102690	AREL1	Intron	Immune system function
cg01112551	ARIH1	Intron	Signaling pathways
cg08747414	CREBRF	Intron	Transcription factor, DNA-binding transcription factor activity
cg02153665	CSDE1	Intron	DNA-binding transcription factor activity
cg02727970	CUNH15orf41	Intron	Immune system function, metabolism
cg27300579	DACH1	Intron	Cold adaptation, DNA-binding transcription factor activity, regulation of gene expression, transcription factor
cg00957561	DOCK1	Intron	Signaling pathways, immune system function, chromatin organization
cg07682092	ELL2	Intron	Histone methylation, regulation of gene expression, signaling pathways, transcription factor
cg20849614	FAF2	Intron	Immune system function, metabolic processes
cg19243601	FBXL20	Intron	Neurotransmitter receptor activity, immune system function
cg01476332	FOSB	Intron	DNA-binding transcription factor activity, hibernation, transcription factor
cg07037105	FOXP1	Intron	DNA-binding transcription factor activity, regulation of gene expression, signaling pathways, immune system function, neurotransmitter receptor activity

cg22457995	GSK3B	Intron	Metabolic processes, signaling pathways, immune system function, hibernation, neurotransmitter
cg09733019	HECTD1	Intron	Immune system function, neurotransmitter receptor activity
cg10400390	KCNMA1	Intron	Neurotransmitter receptor activity, signaling pathways
cg15216075	KLHL14	Intron	Protein coding
cg17464264	LRRC41	Intron	Immune system function
cg14764181	MAPKAP1	Intron	Hibernation, signaling pathways
cg04713622	MAX	Intron	Histone methylation, chromatin organization, DNA-binding transcription factor activity, transcription factor
cg19152246	MBIP	Intron	Histone methylation, chromatin organization
cg01008443	MEGF11	Intron	Signaling pathways
cg05297552	MRM1	Intron	RNA methyltransferase
cg05019226	NQO1	Intron	Oxidoreductase
cg17048874	PAX6	Intron	DNA-binding transcription factor activity, regulation of gene expression, signaling pathways, chromatin organization, transcription factor
cg22377555	PMFBP1	Intron	Cytoskeleton organization
cg11403860	POU3F3	Intron	Transcription factor
cg20817759	PRR5L	Intron	Signaling pathways
cg09760769	PTPN5	Intron	Signaling pathways
cg02437705	TCF7L2	Intron	DNA-binding transcription factor activity, signaling pathways, chromatin organization, transcription factor
cg16009877	UBR3	Intron	DNA-binding transcription factor activity, neurotransmitter receptor activity
cg16518996	ZNF536	Intron	Transcription factor
cg26457089	ADAMTSL1	Exon	Metabolic processes
cg10535197	ADGRB3	Exon	Signaling pathways
cg19426872	ANKRD17	Exon	Signaling pathways, immune system function, DNA-binding transcription factor activity
cg23311800	ARID5A	Exon	Regulation of gene expression, chromatin organization, DNA-binding transcription factor activity, histone methylation, immune system function
cg01019608	ARPP21	Exon	DNA-binding transcription factor activity
cg05724244	BCL11A	Exon	DNA-binding transcription factor activity, neurotransmitter receptor activity, transcription factor

cg27407249	BICD1	Exon	DNA-binding transcription factor activity, chromatin organization, transmembrane transport
cg08125125	CAMKMT	Exon	Signaling pathways
cg12934306	CELSR3	Exon	Signaling pathways
cg25568239	CIR1	Exon	Signaling pathways, histone methylation, DNA-binding transcription factor activity,
cg11087587	CNOT1	Exon	Hibernation, regulation of gene expression
cg17206035	CNOT9	Exon	DNA-binding transcription factor activity, signaling pathways, regulation of gene expression
cg27007550	CSMD2	Exon	Neurotransmitter receptor activity, immune system function
cg21016723	CTDSP2	Exon	Regulation of gene expression, DNA-binding transcription factor activity, neurological transmitter receptor activity
cg14322760	CTNNA2	Exon	Neurotransmitter receptor activity, signaling pathways
cg11866161	CTNNB1	Exon	DNA-binding transcription factor activity, signaling pathways
cg12838514	DCHS1	Exon	Signaling pathways
cg04584667	DCUN1D4	Exon	Histone methylation
cg17507887	DLX6	Exon	DNA-binding transcription factor activity, transcription factor
cg13223250	DNM3	Exon	Signaling pathways, transmembrane transport
cg08716112	EBF1	Exon	DNA-binding transcription factor activity, chromatin organization, transcription factor
cg18681528	EIF4E2	Exon	Signaling pathways
cg00051709	ESRRG	Exon	DNA-binding transcription factor activity, regulation of gene expression, transcription factor
cg16741216	FOXA2	Exon	DNA-binding transcription factor activity, histone methylation, metabolic processes, regulation of gene expression, chromatin organization, transcription factor
cg02577634	FOXJ3	Exon	DNA-binding transcription factor activity, transcription factor
cg12228552	FOXP2	Exon	DNA-binding transcription factor activity
cg07436962	GLYCTK	Exon	Kinase activity
cg18019455	GSX2	Exon	Transcription factor
cg17798626	HERPUD2	Exon	Protein folding
cg20473430	MAML3	Exon	Signaling pathways, DNA-binding transcription factor activity
cg00493297	MCTP1	Exon	Signaling pathways, DNA-binding transcription factor activity

cg11019398	MSX2	Exon	DNA-binding transcription factor activity, transcription factor
cg13212087	MVB12B	Exon	Immune system function
cg03425039	NF1	Exon	Signaling pathways, neurotransmitter receptor activity
cg10136700	NFIA	Exon	DNA-binding transcription factor activity, transcription factor
cg06810228	NR4A2	Exon	DNA-binding transcription factor activity, transcription factor, regulation of gene expression, signaling pathways, hibernation
cg00324422	PDE5A	Exon	Signaling pathways
cg14992370	PICALM	Exon	DNA-binding transcription factor activity
cg15160556	PLPPR2	Exon	Signaling pathways
cg06658439	POLA1	Exon	Metabolic processes, DNA replication
cg04691337	POU2F2	Exon	Metabolic processes, DNA-binding transcription factor activity, transcription factor
cg04833497	POU4F3	Exon	Transcription factor, signaling pathways, neurological transmitter activity
cg04030186	R3HDM1	Exon	DNA-binding transcription factor activity
cg08666298	RBMX	Exon	DNA-binding transcription factor activity, signaling pathways
cg06584607	RPS6KA3	Exon	Signaling pathways, histone modifications
cg16523162	SHISAL2B	Exon	Scaffold/adaptor protein
cg08070857	SKOR2	Exon	DNA-binding transcription factor activity, signaling pathways
cg03458585	TBX4	Exon	DNA-binding transcription factor activity, gene regulation, transcription factor
cg18442187	TFAP2A	Exon	Transcription factor
cg07164816	TLX1	Exon	DNA-binding transcription factor activity, immune system function, neurotransmitter receptor activity, transcription factor
cg15792779	TPM3	Exon	Hibernation
cg01901100	TRIM67	Exon	Metabolic processes
cg11720786	TRIM8	Exon	Immune system function
cg11227540	TRPM7	Exon	Signaling pathways, hibernation
cg17929892	UBFD1	Exon	Metabolic processes
cg22075970	VAMP4	Exon	Transmembrane transport
cg02153512	VPS13B	Exon	Transmembrane transport
cg03830212	VPS37D	Exon	Transmembrane transport
cg25450666	WASF3	Exon	Signaling pathways
cg14323200	WBP1L	Exon	Protein coding
cg25448958	WNT5A	Exon	Signaling pathways, DNA-binding transcription factor activity

cg04287366	ZBTB20	Exon	DNA-binding transcription factor activity, immune system function, neurotransmitter receptor activity, transcription factor
cg03295417	ZBTB44	Exon	DNA-binding transcription factor activity, transcription factor
cg04839060	ZBTB7B	Exon	Metabolic processes, immune system function, cold-adaptation, transcription factor
cg17258599	ZEB2	Exon	DNA-binding transcription factor activity, signaling pathways, transcription factor
cg25908356	ZFHX3	Exon	DNA-binding transcription factor activity, circadian rhythm, neurotransmitter receptor activity, transcription factor
cg12616148	ZNF423	Exon	Transcription factor, DNA-binding transcription factor activity
cg11798921	ZNF608	Exon	DNA-binding transcription factor activity
cg18061345	ARFGEF2	5'UTR	Transmembrane transport
cg00054169	ATP2B2	5'UTR	Signaling pathways
cg25670428	CALU	5'UTR	Signaling pathways
cg05822239	CCDC88A	5'UTR	Signaling pathways, neurotransmitter receptor activity
cg07959695	CLPB	5'UTR	Signaling pathways, immune system function
cg13830021	CLSTN2	5'UTR	Transmembrane transport
cg18028666	ERC2	5'UTR	Signaling pathways, neurotransmitter receptor activity
cg05647280	HOXB3	5'UTR	DNA-binding transcription factor activity, transcription factor
cg02688117	ILF3	5'UTR	Immune system function, DNA-binding transcription factor activity
cg05864181	KLHL32	5'UTR	Protein coding
cg26717518	NAV1	5'UTR	Neurotransmitter receptor activity
cg04827261	OGDH	5'UTR	Metabolic processes, hibernation
cg13055461	PEX14	5'UTR	Signaling pathways, histone methylation, DNA-binding transcription factor activity
cg09548426	PLAG1	5'UTR	DNA-binding transcription factor activity, transcription factor
cg05328510	RALGAPA2	5'UTR	Transmembrane transport
cg01366864	SGPL1	5'UTR	Neurotransmitter receptor activity, metabolic processes
cg24460268	SOX2	5'UTR	Transcription factor
cg12346383	TRPS1	5'UTR	DNA-binding transcription factor activity, regulation of gene expression, transcription factor
cg26679498	AHCYL1	3'UTR	Signaling pathways

cg11657870	CNOT4	3'UTR	DNA-binding transcription factor activity, regulation of gene expression
cg16864011	CNR1	3'UTR	Signaling pathways, regulation of gene expression, metabolic processes, hibernation
cg08696330	COL1A2	3'UTR	Transcription by RNA polymerase II
cg09886289	DGKG	3'UTR	Metabolic processes, signaling pathways
cg03448317	EGLN1	3'UTR	DNA-binding transcription factor activity, signaling pathways
cg17655935	PITX1	3'UTR	DNA-binding transcription factor activity, transcription factor
cg11878585	PRMT3	3'UTR	Chromatin organization, histone methylation
cg20836370	ROBO1	3'UTR	Neurotransmitter receptor activity
cg08208061	SND1	3'UTR	DNA-binding transcription factor activity, immune system function, hibernation

cg03450918	HELT	Intron	Transcription factor, DNA-binding transcription factor activity
cg12457066	INHBB	Intron	Signaling pathway
cg01771997	LIN28A	Intron	Metabolic processes, DNA-binding transcription factor activity, signaling pathways
cg08305550	MVB12B	Intron	Immune system function
cg24495632	MYO18A	Intron	Signaling pathways, immune system function, transcription factor
cg04670975	NEUROD6	Intron	Transcription factor
cg04696116	RFX3	Intron	Transcription factor, DNA-binding transcription factor activity, regulation of gene expression
cg00773909	SATB1	Intron	Transcription factor
cg04222851	TNIK	Intron	Signaling pathways, anatomical structure
cg06900751	TRABD2B	Intron	Signaling pathways
cg22358580	TTN	Intron	Chromatin organization, hibernation, DNA-binding transcription factor activity
cg18033250	TWIST2	Intron	Anatomical structure, DNA-binding transcription factor activity, metabolic process, signaling pathways, transcription factor
cg03275335	UNCX	Intron	Transcription factor
cg08256518	VTI1A	Intron	Transmembrane transport, DNA-binding transcription factor activity
cg15913680	ZC3H12B	Intron	Immune system function, signaling pathways
cg10419473	ATXN7L3	Exon	Chromatin organization, regulation of gene expression, DNA-binding transcription factor activity

cg02739728	BCOR	Exon	DNA-binding transcription factor activity, regulation of gene activity, chromatin organization
cg00583683	CDKN2C	Exon	Cell cycle control
cg09666298	CHD4	Exon	Chromatin organization, histone methylation, DNA-binding transcription factor activity
cg09336476	COL7A1	Exon	Immune system function
cg25828170	DENND5A	Exon	Transmembrane transport, neurological development
cg05450500	EIF5A	Exon	Metabolic processes, anatomical structure
cg02523575	ELAVL4	Exon	Transcription factor, DNA-binding transcription factor activity
cg26647900	EXT1	Exon	Regulation of gene expression
cg20006282	GJD2	Exon	Transmembrane transport
cg21389718	HOXC6	Exon	Transcription factor, DNA-binding transcription factor activity
cg01993707	KCNG3	Exon	Neurological development, signaling pathways
cg08477399	LMO3	Exon	Leukemia
cg11327853	MBTD1	Exon	DNA-binding transcription factor activity, chromatin organization, regulation of gene expression
cg14218309	MEGF11	Exon	Signaling pathways
cg15486257	MRTFA	Exon	Signaling pathways, transcription factor
cg12474251	NEUROD1	Exon	Transcription factor, DNA-binding transcription factor activity
cg06455216	OTP	Exon	DNA-binding transcription factor activity
cg04337454	PCBD2	Exon	Metabolic process, DNA-binding transcription factor activity
cg02135089	PEX14	Exon	Signaling pathways, histone methylation, DNA-binding transcription factor activity
cg04110571	PRUNE2	Exon	Immune system function, signaling pathways
cg20041729	R3HDM2	Exon	DNA-binding transcription factor activity
cg24856447	RARA	Exon	Transcription factor, regulation of gene expression, chromatin organization circadian rhythm, anatomical structure
cg11922307	RGS7	Exon	Signaling pathways
cg13849459	RNF220	Exon	Immune system function, signaling pathways
cg16512330	SIX3	Exon	Transcription factor, DNA-binding transcription factor activity, signaling pathways
cg07576603	SMARCE1	Exon	DNA-binding transcription factor activity, histone methylation regulation of gene of gene expression, signaling pathways, chromatin organization
cg25301626	SOCS3	Exon	Signaling pathways, immune system function
cg13619139	TBCA	Exon	Metabolic processes

cg13200141	TRPS1	Exon	Transcription factor
cg01135274	TTC17	Exon	Anatomical structure
cg18842854	VSNL1	Exon	Signaling pathways, neurological development
cg25352702	ZFHX4	Exon	Transcription factor, DNA-binding transcription factor activity, neurological development
cg09825093	ADAMTS6	5'UTR	Metabolic process
cg03805542	CSDE1	5'UTR	DNA-binding transcription factor activity
cg10858898	GRIA3	5'UTR	Signaling pathways
cg14679255	GSX2	5'UTR	Transcription factor
cg19544104	KDM2A	5'UTR	Chromatin organization, histone methylation, circadian rhythm
cg19799050	NR2E1	5'UTR	DNA-binding transcription factor activity, transcription factor, regulation of gene expression
cg22025436	PAX8	5'UTR	Transcription factor
cg14334667	SOX5	5'UTR	Transcription factor, regulation of gene expression, DNA-binding transcription factor activity
cg23296078	SOX6	5'UTR	Transcription factor, regulation of gene expression, DNA-binding transcription factor activity, anatomical structure
cg05646405	FAP	3'UTR	Immune system function
cg09858514	GLI3	3'UTR	Transcription factor, DNA-binding transcription factor activity
cg11716762	RIOK3	3'UTR	Immune system function, signaling pathways
cg16034392	RSRC1	3'UTR	Alternative mRNA splicing

Appendix D Negative CpG site association in E055 foreskin fibroblast primary skin cell line for the hibernation contrast analysis

CpG site	Symbol	Location	Category
cg19134370	ANO4	Promoter	Transmembrane transport, signaling pathways
cg09731012	BEND4	Promoter	Protein coding
cg18722778	DPYD	Promoter	Metabolic processes
cg18306442	HDAC9	Promoter	Signaling pathways, histone methylation, DNA-binding transcription factor activity
cg15809488	HIPK1	Promoter	Regulation of gene expression
cg02800363	JUND	Promoter	Transcription factor, DNA-binding transcription factor activity, signaling pathways,
cg11351514	MLLT11	Promoter	Leukemia
cg09008979	NR2F2	Promoter	Transcription factor, DNA-binding transcription factor activity
cg26275174	PAX6	Promoter	DNA-binding transcription factor activity, transcription factor, regulation of gene expression, signaling pathways, chromatin organization
cg02119111	PPP4R3A	Promoter	DNA-binding transcription factor activity

cg18994927	TBL1XR1	Promoter	Regulation of gene expression, chromatin organization, circadian rhythm, DNA-binding transcription factor activity
cg02227188	ZEB2	Promoter	DNA-binding transcription factor activity, transcription factor, signaling pathways
cg14341524	ZIC5	Promoter	Transcription factor
cg06663517	ACACA	Intron	Metabolic process, hibernation
cg00519301	BNC2	Intron	Transcription factor, hibernation, neurological development
cg12807727	CELF3	Intron	DNA-binding transcription factor activity
cg14617937	CNOT2	Intron	Transcription factor, regulation of gene expression, DNA-binding transcription factor activity, histone methylation
cg12714873	DTX3	Intron	Signaling pathways, hibernation
cg02715589	EMX2	Intron	Transcription factor
cg05971894	FAF1	Intron	DNA-binding transcription factor activity
cg05584808	FEZF2	Intron	Anatomical structure, DNA-binding transcription factor activity, immune system function, transcription factor
cg01403803	HDAC4	Intron	Histone methylation, DNA-binding transcription factor activity
cg03450918	HELT	Intron	Transcription factor, DNA-binding transcription factor activity
cg08305550	MVB12B	Intron	Immune system function
cg24495632	MYO18A	Intron	Signaling pathways, immune system function, transcription factor
cg04670975	NEUROD6	Intron	Transcription factor
cg00773909	SATB1	Intron	Transcription factor
cg06900751	TRABD2B	Intron	Signaling pathways
cg22358580	TTN	Intron	Chromatin organization, hibernation, DNA-binding transcription factor activity
cg18033250	TWIST2	Intron	Anatomical structure, DNA-binding transcription factor activity, metabolic process, signaling pathways, transcription factor
cg03275335	UNCX	Intron	Transcription factor
cg24357465	WWP2	Intron	Metabolic processes, DNA-binding transcription factor activity, transmembrane transport
cg15913680	ZC3H12B	Intron	Immune system function, signaling pathways
cg20728253	ASF1A	Exon	Histone methylation, chromatin organization
cg10419473	ATXN7L3	Exon	Chromatin organization, regulation of gene expression, DNA-binding transcription factor activity
cg25828170	DENND5A	Exon	Transmembrane transport, neurological development
cg05450500	EIF5A	Exon	Metabolic processes, anatomical structure
cg02523575	ELAVL4	Exon	Transcription factor, DNA-binding transcription factor activity

cg26647900	EXT1	Exon	Regulation of gene expression
cg20006282	GJD2	Exon	Transmembrane transport Transcription factor, DNA-binding transcription factor activity
cg21389718	HOXC6	Exon	Neurological development, signaling pathways
cg01993707	KCNG3	Exon	Leukemia
cg08477399	LMO3	Exon	Signaling pathways, transcription factor
cg15486257	MRTFA	Exon	Transcription factor, DNA-binding transcription factor activity
cg12474251	NEUROD1	Exon	DNA-binding transcription factor activity
cg06455216	OTP	Exon	Metabolic process, DNA-binding transcription factor activity
cg04337454	PCBD2	Exon	Signaling pathways
cg11922307	RGS7	Exon	Immune system function, signaling pathways
cg13849459	RNF220	Exon	Transcription factor, DNA-binding transcription factor activity, signaling pathways
cg16512330	SIX3	Exon	DNA-binding transcription factor activity
cg04148340	SMG1	Exon	Signaling pathways, immune system function
cg25301626	SOCS3	Exon	Metabolic processes
cg13619139	TBCA	Exon	Transcription factor, DNA-binding transcription factor activity, neurological development
cg07670524	ZFHX4	Exon	Metabolic process
cg09825093	ADAMTS6	5'UTR	Signaling pathways
cg10858898	GRIA3	5'UTR	Transcription factor
cg14679255	GSX2	5'UTR	DNA-binding transcription factor activity, Transcription factor, regulation of gene expression
cg19799050	NR2E1	5'UTR	Transcription factor, regulation of gene expression, DNA-binding transcription factor activity
cg14334667	SOX5	5'UTR	Transcription factor, regulation of gene expression, DNA-binding transcription factor activity, anatomical structure
cg23296078	SOX6	5'UTR	Transmembrane transport, DNA-binding transcription factor activity
cg03672541	VTI1A	5'UTR	Immune system function
cg05646405	FAP	3'UTR	Immune system function, signaling pathways
cg11716762	RIOK3	3'UTR	Alternative mRNA splicing
cg16034392	RSRC1	3'UTR	

Bibliography

- Al-attar, R., & Storey, K. B. (2020). Suspended in time: Molecular responses to hibernation also promote longevity. *Experimental Gerontology*, *134*, 110889.
<https://doi.org/10.1016/j.exger.2020.110889>
- Alvarado, S., Mak, T., Liu, S., Storey, K. B., & Szyf, M. (2015). Dynamic changes in global and gene-specific DNA methylation during hibernation in adult thirteen-lined ground squirrels, *Ictidomys tridecemlineatus*. *The Journal of Experimental Biology*, *218*(Pt 11), 1787–1795. <https://doi.org/10.1242/jeb.116046>
- Andrews, M. T. (2019). Molecular interactions underpinning the phenotype of hibernation in mammals. *Journal of Experimental Biology*, *222* (jeb160606).
<https://doi.org/10.1242/jeb.160606>
- Arneson, A., Haghani, A., Thompson, M. J., Pellegrini, M., Kwon, S. B., Vu, H., Li, C. Z., Lu, A. T., Barnes, B., Hansen, K. D., Zhou, W., Breeze, C. E., Ernst, J., & Horvath, S. (2021). A mammalian methylation array for profiling methylation levels at conserved sequences. *BioRxiv*, 2021.01.07.425637. <https://doi.org/10.1101/2021.01.07.425637>
- Bannister, A. J., & Kouzarides, T. (2011). Regulation of chromatin by histone modifications. *Cell Research*, *21*(3), 381–395. <https://doi.org/10.1038/cr.2011.22>
- Ben-Hamo, M., Muñoz-Garcia, A., Williams, J. B., Korine, C., & Pinshow, B. (2013). Waking to drink: Rates of evaporative water loss determine arousal frequency in hibernating bats. *The Journal of Experimental Biology*, *216*(Pt 4), 573–577.
<https://doi.org/10.1242/jeb.078790>
- Benjamini, Y., & Yekutieli, D. (2001). The control of the false discovery rate in multiple testing under dependency. *The Annals of Statistics*, *29*(4), 1165–1188.
<https://doi.org/10.1214/aos/1013699998>

- Biggar, Y., & Storey, K. B. (2014). Global DNA modifications suppress transcription in brown adipose tissue during hibernation. *Cryobiology*, 69(2), 333–338.
<https://doi.org/10.1016/j.cryobiol.2014.08.008>
- Blažek, J., Zukal, J., Bandouchova, H., Berková, H., Kovacova, V., Martínková, N., Pikula, J., Řehák, Z., Škrabánek, P., & Bartonička, T. (2019). Numerous cold arousals and rare arousal cascades as a hibernation strategy in European *Myotis* bats. *Journal of Thermal Biology*, 82, 150–156. <https://doi.org/10.1016/j.jtherbio.2019.04.002>
- Bouma, H. R., Carey, H. V., & Kroese, F. G. M. (2010). Hibernation: The immune system at rest? *Journal of Leukocyte Biology*, 88(4), 619–624. <https://doi.org/10.1189/jlb.0310174>
- Boyer, C., Cussonneau, L., Brun, C., Deval, C., Pais de Barros, J.-P., Chanon, S., Bernoud-Hubac, N., Daira, P., Evans, A. L., Arnemo, J. M., Swenson, J. E., Gauquelin-Koch, G., Simon, C., Blanc, S., Combaret, L., Bertile, F., & Lefai, E. (2020). Specific shifts in the endocannabinoid system in hibernating brown bears. *Frontiers in Zoology*, 17(1), 35.
<https://doi.org/10.1186/s12983-020-00380-y>
- Breeze, C. E., Reynolds, A. P., van Dongen, J., Dunham, I., Lazar, J., Neph, S., Vierstra, J., Bourque, G., Teschendorff, A. E., Stamatoyannopoulos, J. A., & Beck, S. (2019). eFORGE v2.0: Updated analysis of cell type-specific signal in epigenomic data. *Bioinformatics (Oxford, England)*, 35(22), 4767–4769.
<https://doi.org/10.1093/bioinformatics/btz456>
- Calo, E. and Wysocka, J. (2013). Modification of enhancer chromatin: what, how, and why? *Molecular Cell* 49, 825–837. 10.1016/j.molcel.2013.01.038.
- Capraro, A., O’Meally, D., Waters, S. A., Patel, H. R., Georges, A., & Waters, P. D. (2019). Waking the sleeping dragon: Gene expression profiling reveals adaptive strategies of the

hibernating reptile *Pogona vitticeps*. *BMC Genomics*, 20(1), 1–16.

<https://doi.org/10.1186/s12864-019-5750-x>

Capraro, A., O'Meally, D., Waters, S. A., Patel, H. R., Georges, A., & Waters, P. D. (2020).

MicroRNA dynamics during hibernation of the Australian central bearded dragon

(*Pogona vitticeps*). *Scientific Reports*, 10(1), 17854. [https://doi.org/10.1038/s41598-020-](https://doi.org/10.1038/s41598-020-73706-9)

[73706-9](https://doi.org/10.1038/s41598-020-73706-9)

Carey, H. V., Andrews, M. T., & Martin, S. L. (2003). Mammalian hibernation: cellular and

molecular responses to depressed metabolism and low temperature. *Physiological*

Reviews, 83(4), 1153–1181. <https://doi.org/10.1152/physrev.00008.2003>

Cheney, J. A., Allen, J. J., & Swartz, S. M. (2017). Diversity in the organization of elastin

bundles and intramembranous muscles in bat wings. *Journal of Anatomy*, 230(4), 510–

[523. https://doi.org/10.1111/joa.12580](https://doi.org/10.1111/joa.12580)

Cooper, S. T., Sell, S. S., Fahrenkrog, M., Wilkinson, K., Howard, D. R., Bergen, H., Cruz, E.,

Cash, S. E., Andrews, M. T., & Hampton, M. (2016). Effects of hibernation on bone

marrow transcriptome in thirteen-lined ground squirrels. *Physiological Genomics*, 48(7),

[513–525. https://doi.org/10.1152/physiolgenomics.00120.2015](https://doi.org/10.1152/physiolgenomics.00120.2015)

Crawford, F. I. J., Hodgkinson, C. L., Ivanova, E., Logunova, L. B., Evans, G. J., Steinlechner,

S., & Loudon, A. S. I. (2007). Influence of torpor on cardiac expression of genes

involved in the circadian clock and protein turnover in the Siberian hamster

(*Phodopus sungorus*). *Physiological Genomics*, 31(3), 521–530.

<https://doi.org/10.1152/physiolgenomics.00131.2007>

Czenze, Z. J., Park, A. D., & Willis, C. K. R. (2013). Staying cold through dinner: Cold-climate

bats rewarm with conspecifics but not sunset during hibernation. *Journal of*

Comparative Physiology B, 183(6), 859–866. <https://doi.org/10.1007/s00360-013-0753-4>

- Dausmann, K. H., & Glos, J. (2015). No energetic benefits from sociality in tropical hibernation. *Functional Ecology*, 29(4), 498–505. <https://doi.org/10.1111/1365-2435.12368>
- Drew, K. L., Frare, C., & Rice, S. A. (2017). Neural signaling metabolites may modulate energy use in hibernation. *Neurochemical Research*, 42(1), 141–150. <https://doi.org/10.1007/s11064-016-2109-4>
- Eddy, S. F., & Storey, K. B. (2007). P38 MAPK regulation of transcription factor targets in muscle and heart of the hibernating bat, *Myotis lucifugus*. *Cell Biochemistry and Function*, 25(6), 759–765. <https://doi.org/10.1002/cbf.1416>
- Faure, P. A., Re, D. E., & Clare, E. L. (2009). Wound healing in the flight membranes of big brown bats. *Journal of Mammalogy*, 90(5), 1148–1156. <https://doi.org/10.1644/08-MAMM-A-332.1>
- Fedorov, V. B., Goropashnaya, A. V., Stewart, N. C., Tøien, Ø., Chang, C., Wang, H., Yan, J., Showe, L. C., Showe, M. K., & Barnes, B. M. (2014). Comparative functional genomics of adaptation to muscular disuse in hibernating mammals. *Molecular Ecology*, 23(22), 5524–5537. <https://doi.org/10.1111/mec.12963>
- Friedman, J., Hastie, T., & Tibshirani, R. (2010). Regularization Paths for Generalized Linear Models via Coordinate Descent. *Journal of Statistical Software*, 33(1), 1–22.
- Fu, R., Gillen, A. E., Grabek, K. R., Riemondy, K. A., Epperson, L. E., Bustamante, C. D., Hesselberth, J. R., & Martin, S. L. (2021). Dynamic RNA regulation in the brain underlies physiological plasticity in a hibernating mammal. *Frontiers in Physiology*, 11. <https://doi.org/10.3389/fphys.2020.624677>

- Fujii, G., Nakamura, Y., Tsukamoto, D., Ito, M., Shiba, T., & Takamatsu, N. (2006). CpG methylation at the USF-binding site is important for the liver-specific transcription of the chipmunk HP-27 gene. *The Biochemical Journal*, *395*(1), 203–209.
<https://doi.org/10.1042/BJ20051802>
- Grabek, K. R., Martin, S. L., & Hindle, A. G. (2015). Proteomics approaches shed new light on hibernation physiology. *Journal of Comparative Physiology B*, *185*(6), 607–627.
<https://doi.org/10.1007/s00360-015-0905-9>
- Hampton, M., Melvin, R. G., & Andrews, M. T. (2013). Transcriptomic analysis of brown adipose tissue across the physiological extremes of natural hibernation. *PLoS ONE*, *8*(12). <https://doi.org/10.1371/journal.pone.0085157>
- Hashimoto, M., Gao, B., Kikuchi-Utsumi, K., Ohinata, H., & Osborne, P. G. (2002). Arousal from hibernation and BAT thermogenesis against cold: Central mechanism and molecular basis. *Journal of Thermal Biology*, *27*(6), 503–515.
[https://doi.org/10.1016/S0306-4565\(02\)00024-4](https://doi.org/10.1016/S0306-4565(02)00024-4)
- Hindle, A. G., & Martin, S. L. (2013). Intrinsic circannual regulation of brown adipose tissue form and function in tune with hibernation. *American Journal of Physiology-Endocrinology and Metabolism*, *306*(3), E284–E299.
<https://doi.org/10.1152/ajpendo.00431.2013>
- Horvath, S. (2013). DNA methylation age of human tissues and cell types. *Genome Biology*, *14*(10), 3156. <https://doi.org/10.1186/gb-2013-14-10-r115>
- Hrvatin, S., Sun, S., Wilcox, O. F., Yao, H., Lavin-Peter, A. J., Cicconet, M., Assad, E. G., Palmer, M. E., Aronson, S., Banks, A. S., Griffith, E. C., & Greenberg, M. E. (2020). Neurons that regulate mouse torpor. *Nature*, *583*(7814), 115–121.
<https://doi.org/10.1038/s41586-020-2387-5>

- Jansen, H. T., Trojahn, S., Saxton, M. W., Quackenbush, C. R., Hutzenbiler, B. D. E., Nelson, O. L., Cornejo, O. E., Robbins, C. T., & Kelley, J. L. (2019). Hibernation induces widespread transcriptional remodeling in metabolic tissues of the grizzly bear. *Communications Biology*, 2(1), 1–10. <https://doi.org/10.1038/s42003-019-0574-4>
- Jastroch, M., Giroud, S., Barrett, P., Geiser, F., Heldmaier, G., & Herwig, A. (2016). Seasonal control of mammalian energy balance: Recent advances in the understanding of daily torpor and hibernation. *Journal of Neuroendocrinology*, 28(11). <https://doi.org/10.1111/jne.12437>
- Jonasson, K. A., & Willis, C. K. R. (2012). Hibernation energetics of free-ranging little brown bats. *Journal of Experimental Biology*, 215(12), 2141–2149. <https://doi.org/10.1242/jeb.066514>
- Kassambara, A. (2020). rstatix: Pipe-Friendly Framework for Basic Statistical Tests. R package version 0.6.0. <https://CRAN.R-project.org/package=rstatix>
- Klug, B. J., & Brigham, R. M. (2015). Changes to metabolism and cell physiology that enable mammalian hibernation. *Springer Science Reviews*, 3(1), 39–56. <https://doi.org/10.1007/s40362-015-0030-x>
- Lei, M., Dong, D., Mu, S., Pan, Y.H., & Zhang, S. (2014). Comparison of brain transcriptome of the greater horseshoe bats (*Rhinolophus ferrumequinum*) in active and torpid episodes. *PLOS ONE*, 9(9), e107746. <https://doi.org/10.1371/journal.pone.0107746>
- Lin, J. Q., Huang, Y. Y., Bian, M.Y., Wan, Q. H., & Fang, S.-G. (2020). A Unique Energy-Saving Strategy during Hibernation Revealed by Multi-Omics Analysis in the Chinese Alligator. *IScience*, 23(6), 101202. <https://doi.org/10.1016/j.isci.2020.101202>

Local, A., Huang, H., Albuquerque, C.P. Singh, N., Young Lee, A., Wang, W., Wang, C., Hsia, J. E., Shiau, A. K., Ge, K., Corbett, K. D., Wang, D., Zhou, H. & Ren, B. (2018). Identification of H3K4me1-associated proteins at mammalian enhancers. *Nature Genetics*, 50, 73–82. <https://doi.org/10.1038/s41588-017-0015-6>

Lu, A., Fei, Z., Haghani, A., Robeck, T., Zoller, J., Li, C., Zhang, J., Ablaeva, J., Adams, D., Almunia, J., Ardehali, R., Arneson, A., Baker, C. Belov, K., Black, P., Blumstein, D., Bors, D., Breeze, C., Brooke, R., Brown, J., Caulton, A., Cavin, J., Chatzistamou, I., Chen, H., Chiavellini, P., Choi, O., Clarke, S., DeYoung, J., Dold, C., Emmons, C., Emmrich, S., Faulkes, C., Ferguson, S., Finno, C., Gaillard, J., Garde, E., Gladyshev, V., Gorbunova, V., Goya, R., Grant, M., Hales, E., Hanson, M., Haulena, M., Hogan, A., Hogg, C., Hore, T., Jasinska, A., Jones, G., Jourdain, E., Kasphur, O., Katcher, H., Katsimata, E., Kaza, V., Kiaris, H., Kobor, M., Kordowitzki, P., Koski, W., Larison, B., Lee, S., Lee, Y., Lehmann, M., Lemaitre, J., Levine, A., Li, C., Li, X., Lin, D., Macoretta, N., Maddox, D., Matkin, C., Mattison, J., Mergl, J., Meudt, J., Mozhui, K., Naderi, A., Nagy, M., Narayan, P., Nathanielsz, P., Nguyen, N., Niehrs, C., Ophir, A., Ostrander, E., Ginn, P., Parsons, K., Paul, K., Pellegrini, M., Pinho, G., Plassaos, Prado, N., Rey, B., Ritz, B., Robbins, J., Rodriguez, M., Russell, J., Rydkina, E., Sailer, Salmon, A., Sanghavi, A., Schachtschneider, K., Schmitt, D., Schmitt, T., Schomacher, L., Schook, L., Sears, K., Seluanov, A., Shanmuganayagam, D., Shindyapina, A., Singh, K., Sinha, I., Snell, R., Soltanmaohammadi, E., Spangler, M., Staggs, L., Steinman, K., Sugrue, V., Szladovits, B., Takasugi, M., Teeling, E., Thompson, M., Vann Bonn, B., Vernes, S., Villar, D., Vinters, H., Wallingford, Wang, N., Wayne, R., Wilkinson, G., Williams, C., Williams, R., Yang, X., Young, B., Zhang, B., Zhang, Z., Zhao, P., Zhao, Y., Zimmermann, J., Zhou, W., Ernst, J., Raj, K., Horvath, S. (2021). Universal DNA

methylation age across mammalian tissues. *BioRxiv*, 2021.01.19. 426733.

<https://doi.org/10.1101/2021.01.18.426733>

Luu, B. E., Biggar, K. K., Wu, C.-W., & Storey, K. B. (2016). Torpor-responsive expression of novel microRNA regulating metabolism and other cellular pathways in the thirteen-lined ground squirrel, *Ictidomys tridecemlineatus*. *FEBS Letters*, 590(20), 3574–3582.

<https://doi.org/10.1002/1873-3468.12435>

Mi, H., Ebert, D., Muruganujan, A., Mills, C., Albu, L.-P., Mushayamaha, T., and Thomas, P. D. (2020). PANTHER version 16: A revised family classification, tree-based classification tool, enhancer regions and extensive API. *Nucleic Acids Research*, 49(D1), D394–D403. <https://doi.org/10.1093/nar/gkaa1106>

Monroy, J. A., Carter, M. E., Miller, K. E., & Covey, E. (2011). Development of echolocation and communication vocalizations in the big brown bat, *Eptesicus fuscus*. *Journal of Comparative Physiology. A, Neuroethology, Sensory, Neural, and Behavioral Physiology*, 197(5), 459–467. <https://doi.org/10.1007/s00359-010-0614-5>

Moore, L. D., Le, T., & Fan, G. (2013). DNA Methylation and Its Basic Function.

Neuropsychopharmacology, 38(1), 23–38. <https://doi.org/10.1038/npp.2012.112>

Mugahid, D. A., Sengul, T. G., You, X., Wang, Y., Steil, L., Bergmann, N., Radke, M. H., Ofenbauer, A., Gesell-Salazar, M., Balogh, A., Kempa, S., Tursun, B., Robbins, C. T., Völker, U., Chen, W., Nelson, L., & Gotthardt, M. (2019). Proteomic and Transcriptomic Changes in Hibernating Grizzly Bears Reveal Metabolic and Signaling Pathways that Protect against Muscle Atrophy. *Scientific Reports*, 9(1), 19976.

<https://doi.org/10.1038/s41598-019-56007-8>

- Musselman, C. A., Lalonde, M.-E., Côté, J., & Kutateladze, T. G. (2012). Perceiving the epigenetic landscape through histone readers. *Nature Structural & Molecular Biology*, *19*(12), 1218–1227. <https://doi.org/10.1038/nsmb.2436>
- Nespolo, R. F., Gaitan-Espitia, J. D., Quintero-Galvis, J. F., Fernandez, F. V., Silva, A. X., Molina, C., Storey, K. B., & Bozinovic, F. (2018). A functional transcriptomic analysis in the relict marsupial *Dromiciops gliroides* reveals adaptive regulation of protective functions during hibernation. *Molecular Ecology*, *27*(22), 4489–4500. <https://doi.org/10.1111/mec.14876>
- Outchkourov, N. S., Muiño, J. M., Kaufmann, K., van Ijcken, W. F. J., Groot Koerkamp, M. J., van Leenen, D., de Graaf, P., Holstege, F. C. P., Grosveld, F. G., & Timmers, H. T. M. (2013). Balancing of histone H3K4 methylation states by the Kdm5c/SMCX histone demethylase modulates promoter and enhancer function. *Cell Reports*, *3*(4), 1071–1079. <https://doi.org/10.1016/j.celrep.2013.02.030>
- Pan, Y.-H., Zhang, Y., Cui, J., Liu, Y., McAllan, B. M., Liao, C.-C., & Zhang, S. (2013). Adaptation of phenylalanine and tyrosine catabolic pathway to hibernation in bats. *PLoS ONE*, *8*(4). <https://doi.org/10.1371/journal.pone.0062039>
- Pinho, G. M., Martin, J. G. A., Farrell, C., Haghani, A., Zoller, J. A., Zhang, J., Snir, S., Pellegrini, M., Wayne, R. K., Blumstein, D. T., & Horvath, S. (2021). Hibernation slows epigenetic aging in yellow-bellied marmots. *BioRxiv*, 2021.03.07.434299. <https://doi.org/10.1101/2021.03.07.434299>
- R Core Team (2020). R: A language and environment for statistical computing. R Foundation for Statistical Computing, Vienna, Austria. URL: <https://www.R-project.org/>.

- Rakyan, V. K., Down, T. A., Maslau, S., Andrew, T., Yang, T.-P., Beyan, H., Whittaker, P., McCann, O. T., Finer, S., Valdes, A. M., Leslie, R. D., Deloukas, P., & Spector, T. D. (2010). Human aging-associated DNA hypermethylation occurs preferentially at bivalent chromatin domains. *Genome Research*, *20*(4), 434–439. <https://doi.org/10.1101/gr.103101.109>
- Razin, A., & Riggs, A. D. (1980). DNA methylation and gene function. *Science (New York, N.Y.)*, *210*(4470), 604–610. <https://doi.org/10.1126/science.6254144>
- Rose, N. R., & Klose, R. J. (2014). Understanding the relationship between DNA methylation and histone lysine methylation. *Biochimica Et Biophysica Acta*, *1839*(12), 1362–1372. <https://doi.org/10.1016/j.bbagr.2014.02.007>
- Rouble, A. N., Tessier, S. N., & Storey, K. B. (2014). Characterization of adipocyte stress response pathways during hibernation in thirteen-lined ground squirrels. *Molecular and Cellular Biochemistry*, *393*(1), 271–282. <https://doi.org/10.1007/s11010-014-2070-y>
- Santa Pau, E. C., Real, F. X., & Valencia, A. (2014). Chapter 5—Bioinformatics Analysis of Pancreas Cancer Genome in High-Throughput Genomic Technologies. In A. S. Azmi (Ed.), *Molecular Diagnostics and Treatment of Pancreatic Cancer* (pp. 93–131). Academic Press. <https://doi.org/10.1016/B978-0-12-408103-1.00005-4>
- Shayevitch, R., Askayo, D., Keydar, I., & Ast, G. (2018). The importance of DNA methylation of exons on alternative splicing. *RNA*, *24*(10), 1351–1362. <https://doi.org/10.1261/rna.064865.117>
- Stieler, J. T., Bullmann, T., Kohl, F., Tøien, Ø., Brückner, M. K., Härtig, W., Barnes, B. M., & Arendt, T. (2011). The Physiological Link between Metabolic Rate Depression and Tau Phosphorylation in Mammalian Hibernation. *PLOS ONE*, *6*(1), e14530.

<https://doi.org/10.1371/journal.pone.0014530>

Szereszewski, K. E., & Storey, K. B. (2019). Identification of a prosurvival neuroprotective mitochondrial peptide in a mammalian hibernator. *Cell Biochemistry and Function*, 37(7), 494–503. <https://doi.org/10.1002/cbf.3422>

Tessier, S. N., & Storey, K. B. (2014). To be or not to be: The regulation of mRNA fate as a survival strategy during mammalian hibernation. *Cell Stress & Chaperones*, 19(6), 763–776. <https://doi.org/10.1007/s12192-014-0512-9>

Turbill, C., Bieber, C., & Ruf, T. (2011). Hibernation is associated with increased survival and the evolution of slow life histories among mammals. *Proceedings of the Royal Society B: Biological Sciences*. 278. 1723.

<http://royalsocietypublishing.org/doi/abs/10.1098/rspb.2011.0190>

Unnikrishnan, A., Hadad, N., Masser, D. R., Jackson, J., Freeman, W. M., & Richardson, A. (2018). Revisiting the genomic hypomethylation hypothesis of aging. *Annals of the New York Academy of Sciences*, 1418(1), 69–79. <https://doi.org/10.1111/nyas.13533>

Uzenbaeva, L. B., Belkin, V. V., Ilyukha, V. A., Kizhina, A. G., & Yakimova, A. E. (2015). Profiles and morphology of peripheral blood cells in three bat species of Karelia during hibernation. *Journal of Evolutionary Biochemistry and Physiology*, 51(4), 342–348.

<https://doi.org/10.1134/S0022093015040109>

Vermillion, K. L., Anderson, K. J., Hampton, M., & Andrews, M. T. (2015). Gene expression changes controlling distinct adaptations in the heart and skeletal muscle of a hibernating mammal. *Physiological Genomics*, 47(3), 58–74.

<https://doi.org/10.1152/physiolgenomics.00108.2014>

- Wade, P. A. (2001). Methyl CpG-binding proteins and transcriptional repression. *BioEssays: News and Reviews in Molecular, Cellular and Developmental Biology*, 23(12), 1131–1137. <https://doi.org/10.1002/bies.10008>
- Wang, T., Ma, J., Hogan, A. N., Fong, S., Licon, K., Tsui, B., Kreisberg, J. F., Adams, P. D., Carvunis, A.-R., Bannasch, D. L., Ostrander, E. A., & Ideker, T. (2020). Quantitative translation of dog-to-human aging by conserved remodeling of the DNA methylome. *Cell Systems*, 11(2), 176-185.e6. <https://doi.org/10.1016/j.cels.2020.06.006>
- Wilkinson, G. S., & Adams, D. M. (2019). Recurrent evolution of extreme longevity in bats. *Biology Letters*, 15(4), 20180860. <https://doi.org/10.1098/rsbl.2018.0860>
- Wilkinson, G. S., Adams, D. M., Haghani, A., Lu, A. T., Zoller, J., Breeze, C. E., Arnold, B. D., Ball, H. C., Carter, G. G., Cooper, L. N., Dechmann, D. K. N., Devanna, P., Fasel, N. J., Galazyuk, A. V., Günther, L., Hurme, E., Jones, G., Knörnschild, M., Lattenkamp, E. Z., Li, C. Z., Mayer, F., Reinhardt, J. A., Medellin, R. A., Nagy, M., Pope, B., Power, M. L., Ransome, R. D., Reinhardt, J. A., Teeling, E. C., Vernes, S., C., Zamora-Mejías, D., Zhange, J., Zoller, J., Horvath, S. (2021). DNA methylation predicts age and provides insight into exceptional longevity of bats. *Nature Communications*, 12(1), 1615. <https://doi.org/10.1101/2020.09.04.283655>
- Wilkinson, G. S., & South, J. M. (2002). Life history, ecology and longevity in bats. *Aging Cell*, 1(2), 124–131. <https://doi.org/10.1046/j.1474-9728.2002.00020.x>
- Williams, D. R., Epperson, L. E., Li, W., Hughes, M. A., Taylor, R., Rogers, J., Martin, S. L., Cossins, A. R., & Gracey, A. Y. (2005). Seasonally hibernating phenotype assessed through transcript screening. *Physiological Genomics*, 24(1), 13–22. <https://doi.org/10.1152/physiolgenomics.00301.2004>

- Williams, R. C., Blanco, M. B., Poelstra, J. W., Hunnicutt, K. E., Comeault, A. A., & Yoder, A. D. (2020). Conservation genomic analysis reveals ancient introgression and declining levels of genetic diversity in Madagascar's hibernating dwarf lemurs. *Heredity*, *124*(1), 236–251. <https://doi.org/10.1038/s41437-019-0260-9>
- Willis, C. K. R. (2017). Trade-offs influencing the physiological ecology of hibernation in temperate-zone bats. *Integrative and Comparative Biology*, *57*(6), 1214–1224. <https://doi.org/10.1093/icb/ix087>
- Wu, C.W., Biggar, K. K., Luu, B. E., Szereszewski, K. E., & Storey, K. B. (2016). Analysis of microRNA expression during the torpor-arousal cycle of a mammalian hibernator, the 13-lined ground squirrel. *Physiological Genomics*, *48*(6), 388–396. <https://doi.org/10.1152/physiolgenomics.00005.2016>
- Wu, C.W., & Storey, K. B. (2014). FoxO3a-mediated activation of stress responsive genes during early torpor in a mammalian hibernator. *Molecular and Cellular Biochemistry*, *390*(1), 185–195. <https://doi.org/10.1007/s11010-014-1969-7>
- Wu, C. W., & Storey, K. B. (2018). Regulation of Smad mediated microRNA transcriptional response in ground squirrels during hibernation. *Molecular and Cellular Biochemistry*, *439*(1), 151–161. <https://doi.org/10.1007/s11010-017-3144-4>
- Yin, Q., Ge, H., Liao, C.-C., Liu, D., Zhang, S., & Pan, Y.-H. (2016). Antioxidant Defenses in the Brains of Bats during Hibernation. *PLoS ONE*, *11*(3). <https://doi.org/10.1371/journal.pone.0152135>
- Yin, Q., Zhang, Y., Dong, D., Lei, M., Zhang, S., Liao, C.-C., & Pan, Y.H. (2017). Maintenance of neural activities in torpid *Rhinolophus ferrumequinum* bats revealed by 2D gel-based proteome analysis. *Biochimica et Biophysica Acta (BBA) - Proteins and Proteomics*, *1865*(8), 1004–1019. <https://doi.org/10.1016/j.bbapap.2017.04.006>

- Zhang, W., Ji, W., Yang, J., Yang, L., Chen, W., & Zhuang, Z. (2008). Comparison of global DNA methylation profiles in replicative versus premature senescence. *Life Sciences*, 83(13), 475–480. <https://doi.org/10.1016/j.lfs.2008.07.015>
- Zhou, W., Triche, T. J. Jr., Laird, P. W. & Shen, H. (2018). SeSAmE: reducing artifactual detection of DNA methylation by Infinium BeadChips in genomic deletions. *Nucleic Acids Res.* 46, e123 doi: 10.1093/nar/gky691